Hepatology Publish Ahead of Print
DOI:10.1097/HEP.0000000000000376

OPEN

Downloaded from http://journals.lww.com/hep by BhDMf5ePHKav1zEoum1tQfN4a+kJLhEZgbsIHo4XMi0hCywCX1AWnYQp/IlQrHD3i3D0OdRyi7TvSFl4Cf3VC4/OAVpDDa8K2+Ya6H515kE= on 04/04/2023

A3907, a systemic ASBT inhibitor, improves cholestasis in mice by multi-organ activity and shows translational relevance to humans

Francisco J. Caballero-Camino,[1,2] Pedro M. Rodrigues,[1,3,4] Fredrik Wångsell,[5] Aloña Agirre-Lizaso,[1] Paula Olaizola,[1,3] Laura Izquierdo-Sanchez,[1,3] Maria J. Perugorria,[1,2,3] Luis Bujanda,[1,2,3] Bo Angelin,[6] Sara Straniero,[6] Anna Wallebäck,[5] Ingemar Starke,[5] Per-Göran Gillberg,[5] Ellen Strängberg,[5] Britta Bonn,[5] Jan P. Mattsson,[5] Martin R. Madsen,[7] Henrik H. Hansen,[7] Erik Lindström,[5]* Peter Åkerblad,[5]* Jesus M. Banales.[1,3,4,8]*

[1]Department of Liver and Gastrointestinal Diseases, Biodonostia Health Research Institute – Donostia University Hospital, University of the Basque Country (UPV/EHU), San Sebastian, Spain; [2]Department of Medicine, Faculty of Medicine and Nursing, University of the Basque Country UPV/EHU, Leioa, Spain; [3]National Institute for the Study of Liver and Gastrointestinal Diseases (CIBERehd, "Instituto de Salud Carlos III"), Madrid, Spain; [4]Ikerbasque, Basque Foundation for Science, Bilbao, Spain; [5]Albireo AB, Göteborg, Sweden; [6]CardioMetabolic Unit, Department of Medicine and Clinical Department of Endocrinology, Karolinska Institutet at Karolinska University Hospital Huddinge, Stockholm, Sweden; [7]Gubra, Hoersholm, Denmark; [8]Department of Biochemistry and Genetics, School of Sciences, University of Navarra, Pamplona, Spain.

ACCEPTED

Copyright © 2023 The Author(s). Published by Wolters Kluwer Health, Inc. This is an open access article distributed under the terms of the Creative Commons Attribution-Non Commercial-No Derivatives License 4.0 (CCBY-NC-ND), where it is permissible to download and share the work provided it is properly cited. The work cannot be changed in any way or used commercially without permission from the journal.

* Shared senior authorship

Keywords: ASBT, cholestatic liver disease, pathogenesis, bile acids, precision medicine.

Correspondence: Prof. Jesus M. Banales, PhD, Department of Liver and Gastrointestinal Diseases, Biodonostia Health Research Institute – Donostia University Hospital, Paseo del Dr. Begiristain s/n, E-20014, San Sebastian, Spain. Email: jesus.banales@biodonostia.org/ Phone: +34 943006067; or Peter Åkerblad (peter.akerblad@albireopharma.com); or Erik Lindström (erik.lindstrom@albireopharma.com).

Abbreviations: ANOVA, one-way analysis of variance; ALP, alkaline phosphatase; ALT, alanine aminotransferase; ASBT, apical sodium-dependent bile acid transporter; ASBTi, ASBT inhibitor; α-SMA, α-Smooth muscle actin; AST, aspartate aminotransferase; ATCC, American Type Culture Collection; AUC_{inf}, area under the curve from the time of dosing to the last measurable concentration and extrapolated to infinity; BAs, bile acids; BDL, bile-duct ligated; BSEP, ATP-dependent bile salt export pump; C4, 7α-hydroxy-4-cholesten-3-one; CA, cholic acid; CDCA, chenodeoxycholic acid; C_{max}, maximum plasma concentrations; CMC, carboxymethylcellulose; CK7, cytokeratin-7; Cyp7a1, cytochrome P450 family 7 subfamily A member 1; DCA, deoxycholic acid; DEGs, differentially expressed genes; FFPE, formalin-fixed and paraffin-embedded; GO, gene ontology; HDL, high density lipoproteins; H&E, hematoxylin-eosin; h, hours; IC_{50}, half maximal inhibitory concentration; LCA, lithocholic acid LC-MS/MS, liquid chromatography tandem mass spectrometry; LDL,

Downloaded from http://journals.lww.com/hep by BhDMf5ePHKav1zEoum1tQfN4a+kJLhEZgbsIHo4XMi0hCywCX1AWnYQp/IlQrHD3i3D0OdRyi7TvSFl4Cf3VC4/OAVpDDa8K2+Ya6H515kE= on 04/04/2023

ACCEPTED

low density lipoproteins; MAD, multiple-ascending-dose, placebo-controlled study; MCA, muricholic acids; MCP-1, monocyte chemoattractant protein-1; MDR3, multidrug resistance protein 3; min, minutes; MMP-7, matrix metalloproteinase 7; NRC, normal rat cholangiocytes; NTCP, Na^+-taurocholate co-transport polypeptide; OATP, organic anion transporting polypeptides; OSTα/OSTβ, organic solute transporter alpha/beta; PBC, primary biliary cholangitis; PET, positron emission tomography; PSC, primary sclerosing cholangitis; QWBA, quantitative whole-body autoradiography; RNAseq, RNA sequencing; RT-qPCR, quantitative real time polymerase chain reaction; SAD, single-ascending-dose, placebo-controlled study; SD, standard deviation; sec, seconds; SEM, standard error of the mean; Slc10a2, solute carrier family 10 member 2; $t_{1/2}$, terminal half-life; TEAEs, treatment-emergent adverse events; TIMP-1, metalloproteinase inhibitor 1; T_{max}, time to reach the maximum concentrations; UDCA, ursodeoxycholic acid.

Conflicts of interest:

Fredrik Wångsell consults for Albireo. Bo Angelin consults and received grants from AstraZeneca and Albireo. He received grants from Amgen. Sara Straniero received grants from Albireo. Anna Wallebäck is employed by and owns stock in Albireo. Ingemar Starke is employed by and owns stock in Albireo. Per-Göran Gillberg was previously employed at Albireo. Ellen Strängberg is employed by and owns stock in Albireo. Britta Bonn is employed by and owns stock in Albireo.Jan P. Mattsson is employed by and owns stock in Albireo. Martin R. Madsen is employed by Gubra. Henrik H. Hansen is employed by Gubra. Erik Lindström is employed by and owns stock in Albireo. Peter Åkerblad is employed by and owns stock in Albireo. Jesus M. Banales consults for and received grants from Albireo. He received lecture fees and

Downloaded from http://journals.lww.com/hep by BhDMf5ePHKav1zEoum1tQfN4a+kJLhEZgbsIHo4XMi0hCywCX1AWnYQp/IlQrHD3i3D0OdRyi7TvSFl4Cf3VC4/OAVpDDa8K2+Ya6H515kE= on 04/04/2023

ACCEPTED

grants from Incyte. He consults for QED Therapeutics, OWL Metabolomics, CYMABAY Therapeutics, and Ikan Biotech. He received lecture fees from Intercept. The remaining authors have no conflicts to report.

Downloaded from http://journals.lww.com/hep by BhDMf5ePHKav1zEoum1tQfN4a+kJLhEZgbsIHo4XMi0hCywCX1AWnYQp/IlQrHD3i3D0OdRyi7TvSFl4Cf3VC4/OAVpDDa8K2+Ya6H515kE= on 04/04/2023

Grant Support: Spanish Carlos III Health Institute (ISCIII) [J.M. Banales (FIS PI18/01075, PI21/00922 and Miguel Servet Program CPII19/00008); M.J. Perugorria (FIS PI14/00399, PI17/00022 and PI20/00186); P.M. Rodrigues (Sara Borrell CD19/00254 and Miguel Servet Program CP22/00073)] cofinanced by "*Fondo Europeo de Desarrollo Regional*" (FEDER); "*Instituto de Salud Carlos III*" [CIBERehd: J.M. Banales, M.J. Perugorria, P.M. Rodrigues and L. Bujanda], Spain; Department of Health of the Basque Country (M.J. Perugorria: 2019111024 and J.M. Banales: 2021111021), "*Euskadi RIS3*" (J.M. Banales: 2019222054, 2020333010, 2021333003), and Department of Industry of the Basque Country (J.M. Banales: Elkartek: KK-2020/00008); La Caixa Scientific Foundation (J.M. Banales: HR17-00601); European Union Horizon 2020 Research and Innovation Program (J.M. Banales: grant number 825510, ESCALON). M.J. Perugorria was funded by the Spanish Ministry of Economy and Competitiveness (MINECO: "*Ramón y Cajal*" Programme RYC-2015-17755), A. Agirre-Lizaso by the Basque Government (PRE_2018_1_0184), and FJ Caballero-Camino by the Spanish Ministry of Universities and European Union-Next Generation EU (MARSA21/17, University of Basque Country). IKERBASQUE, Basque foundation for science (to J.M. Banales and P.M. Rodrigues); "Diputación Foral Gipuzkoa" (2020-CIEN-000067-01 and 2021-CIEN-000029-04-01 to P.M. Rodrigues). Project support from the Swedish Heart-Lung Foundation, Stockholm

ACCEPTED

Region/Karolinska Institutet (ALF, CIMED) (to Bo Angelin), and the Swedish Foundation for Strategic Research (to Sara Straniero).

The funding sources had no involvement in study design, data collection and analysis, decision to publish, or preparation of the article.

Author Contributions: FJC-C, PGG, ES, FW, JPM, EL, PA, JMB: study concept and design, analysis and interpretation of data, drafting of the manuscript, review and editing. AW: monitoring the clinical study. HHH, BA, SS, IS: analysis and interpretation of data, drafting of the manuscript, review and editing. FJC-C, PMR, AA-L, PO, LI-S, MJP, LB: acquisition of data. FJC-C, JMB: statistical analysis. EL, PA, BA, SS, JMB: obtained funding. All authors have read and agreed to the final version of the manuscript.

Word count excluding title page, abstract and figure legends: 6224

Number of Figures: 7 (1A-D, 2A-F, 3A-E, 4A-F, 5A-D, 6A-D, 7A-D)

Downloaded from http://journals.lww.com/hep by BhDMf5ePHKav1zEoum1tQfN4a+kJLhEZgbsIHo4XMi0hCywCX1AWnYQp/IlQrHD3i3D0OdRyi7TvSFl4Cf3VC4/OAVpDDa8K2+Ya6H515kE= on 04/04/2023

ACCEPTED

Graphic abstract

Downloaded from http://journals.lww.com/hep by BhDMf5ePHKav1zEoum1tQfN4a+kJLhEZgbsIHo4XMi0hCywCX1AWnYQp/IlQrHD3i3D0OdRyi7TvSFl4Cf3VC4/OAVpDDa8K2+Ya6H515kE= on 04/04/2023

ACCEPTED

Downloaded from http://journals.lww.com/hep by BhDMf5ePHKav1zEoum1tQfN4a+kJLhEZgbsIHo4XMi0hCywCX1AWnYQp/IlQrHD3i3D0OdRyi7TvSFl4Cf3VC4/OAVpDDa8K2+Ya6H515kE= on 04/04/2023

ACCEPTED

Abstract (242 words)

Background & Aims: Cholestasis is characterized by intrahepatic accumulation of bile constituents, including bile acids (BAs), which promote liver damage. The apical sodium-dependent BA transporter (ASBT) plays an important role in BA reabsorption and signaling in ileum, bile ducts and kidneys. Our aim was to investigate the pharmacokinetics and pharmacological activity of A3907, an oral and systemically-available ASBT inhibitor in experimental mouse models of cholestasis. Additionally, the tolerability, pharmacokinetics, and pharmacodynamics of A3907 were examined in healthy humans.

Approach & Results: A3907 was a potent and selective ASBT inhibitor *in vitro.* In rodents, orally-administered A3907 distributed to the ASBT-expressing organs ileum, liver and kidneys, and dose-dependently increased fecal BA excretion. A3907 improved biochemical, histological and molecular markers of liver and bile duct injury in *Mdr2*$^{-/-}$ mice, and also provided direct protective effects on rat cholangiocytes exposed to cytotoxic BA concentrations *in vitro.* In bile-duct ligated mice, A3907 increased urinary BA elimination, reduced serum BA levels and prevented body weight loss, while improving markers of liver injury. A3907 was well-tolerated and demonstrated target engagement in healthy volunteers. Plasma exposure of A3907 in humans was within the range of systemic concentrations that achieved therapeutic efficacy in mouse.

Conclusions: The systemic ASBT inhibitor A3907 improved experimental cholestatic disease by targeting ASBT function at the intestinal, liver and kidney levels, resulting in marked clearance of circulating BAs and liver protection. A3907 is well-tolerated in humans, supporting further clinical development for the treatment of cholestatic liver diseases.

Downloaded from http://journals.lww.com/hep by BhDMf5ePHKav1zEoum1tQfN4a+kJLhEZgbsIHo4XMi0hCywCX1AWnYQp/IlQrHD3i3D0OdRyi7TvSFl4Cf3VC4/OAVpDDa8K2+Ya6H515kE= on 04/04/2023

ACCEPTED

Introduction

Cholestasis is a severe clinical manifestation of adult and pediatric cholangiopathies of diverse etiologies, including genetic, obstructive, drug-induced, or immune-mediated biliary diseases.(1,2) Cholestasis is characterized by decreased or obstructed bile flow leading to hepatic accumulation of bile acids (BAs) and other bile-derived toxic substances, frequently inducing pruritus.(3,4) Cholestatic liver diseases lack effective treatments and can progress to advanced stages (*i.e.*, cirrhosis), increasing the risk for developing hepatobiliary malignancies and liver failure.(5,6)

In human cholangiopathies, alterations in BA synthesis, biotransformation and/or transport may result in pathological conditions, including severe cholestasis and end-stage liver disease, where liver transplantation remains as the only potential curative option. Under physiological conditions, a major fraction of the BAs reaching the intestine (□95%) is efficiently recovered and re-circulated to the liver via the portal vein. This occurs through a complex process involving several BA transporters expressed in different cell types.(7,8) The apical sodium-dependent BA transporter (ASBT), highly expressed in the apical membrane of ileal enterocytes, plays a major role in the reabsorption of BAs from the intestinal lumen, and thus for the regulation of BA dynamics and homeostasis.(7) Interestingly, ASBT is also expressed in the bile ducts and renal proximal tubuli.(9) However, the biliary and renal role of ASBT is less clear and may involve cholehepatic shunting and/or cholangiocyte signalling, as well as renal reabsorption of BAs from filtered primary urine.(10)

Serum BAs are typically elevated in cholestasis reflecting hepatic BA overload.(11) The high levels of BAs in cholestatic liver diseases lead to damage in the liver parenchyma which may ultimately also extend to extrahepatic tissues. In this regard, highly efficient ASBT-driven reabsorption of BAs in the intestine and kidneys

Downloaded from http://journals.lww.com/hep by BhDMf5ePHKav1zEoum1tQfN4a+kJLhEZgbsIHo4XMi0hCywCX1AWnYQp/IlQrHD3i3D0OdRyi7TvSFl4Cf3VC4/OAVpDDa8K2+Ya6H515kE= on 04/04/2023

ACCEPTED

significantly contribute to disease progression and severity. ASBT inhibitors (ASBTi) with restricted intestinal activity in humans have therefore been developed and found useful in several cholestatic conditions by reducing BA load.(12–16) However, due to minimal systemic bioavailability of currently available ASBTis, the therapeutic potential of multi-organ ASBT inhibition for the treatment of different forms of cholestasis has not been explored.

Herein, we hypothesize that multi-organ targeting of ASBT, including the ileum, bile ducts, and renal proximal tubuli, may halt or reverse the progression of cholestatic diseases. This approach might be potentially superior to locally acting ASBTis in severe cholestatic conditions where enterohepatic circulation of BAs is severely compromised. Therefore, the current study aimed to investigate the molecular and *in vivo* pharmacology of the novel orally bioavailable ASBTi A3907 in well-characterized experimental models of cholestatic liver disease (*i.e.*, *Mdr2*$^{-/-}$ mice and mice subjected to bile-duct ligation (BDL)),(17) and investigate its tolerability, oral bioavailability, and pharmacodynamics in healthy human subjects.

Materials and methods

A3907 activity and selectivity *in vitro*

Mouse and human ASBT and NTCP transporters were experimentally overexpressed with recombinant plasmids in CHOK1 hamster ovary cells obtained from the American Type Culture Collection (ATCC). Further experimental details are provided in Supplementary Material http://links.lww.com/HEP/F6.

Quantitative whole-body autoradiography

Downloaded from http://journals.lww.com/hep by BhDMf5ePHKav1zEoum1tQfN4a+kJLhEZgbsIHo4XMi0hCywCX1AWnYQp/IlQrHD3i3D0OdRyi7TvSFl4Cf3VC4/OAVpDDa8K2+Ya6H515kE= on 04/04/2023

Quantitative whole-body autoradiography (QWBA) in phosphor screens was performed using male rats administrated a single oral dose of radiolabeled [^{14}C]-A3907 or a gut-restricted ASBT inhibitor [^{14}C]-A3309(18) with 10 MBq/kg and 7.8 MBq/kg radioactive doses, respectively. Experimental details are provided in Supplementary Material http://links.lww.com/HEP/F6.

A3907 pharmacokinetics and biodistribution in mice and rats

The oral pharmacokinetic profile of A3907 in normal animals was analyzed in three rodent studies (Envigo Research Laboratories): *i*) male Hsd:ICR (CD-1) adult mice, *ii*) male C57BL/6J adult mice, and *iii*) male adult Wistar rats. A3907 biodistribution was analyzed by liquid chromatography tandem mass spectrometry (LC-MS/MS) in samples from male C57BL/6J mice (7 weeks of age) (Janvier Labs) treated with daily doses of A3907 (3, 10, or 30 mg/kg; n=10 per group) by oral gavage for 7 days. The oral pharmacokinetic profile of A3907 and A3309 was analyzed at Syngene International Ltd. (Bangalore, India) in male adult C57BL/6 mice (Hylasco, Hyderabad) subjected to BDL surgery. Fecal BA content following 7-day treatment of A3907, A3309 or vehicle was also analyzed. Further experimental details are provided in Supplementary Material http://links.lww.com/HEP/F6.

Pharmacodynamic studies in normal wild-type mice

Pharmacodynamic studies were performed in adult (13-14 weeks) C57BL/6N mice (Hylasco, Hyderabad, India) administered daily doses of A3907 or A3309 at 3 or 10 mg/kg/day, or vehicle (0.5% carboxymethylcellulose (CMC) + 0.1% Tween 80)] by

ACCEPTED

oral gavage for 8 days. Detailed information provided in Supplementary Material http://links.lww.com/HEP/F6.

Downloaded from http://journals.lww.com/hep by BhDMf5ePHKav1zEoum1tQfN4a+kJLhEZgbsIHo4XMi0hCywCX1AWnYQp/IlQrHD3i3D0OdRyi7TvSFl4Cf3VC4/OAVpDDa8K2+Ya6H515kE= on 04/04/2023

Toxicology studies of A3907 in normal rats

Systemic toxicity was evaluated in Wistar Han Rats (Charles River). 7–10-week-old male (n=76) or female (n=76) rats were administered daily oral doses of A3907 (25, 150 and 1000 mg/kg/day) for 13 weeks by oral gavage. Animals were euthanized, and samples from a standard set of organs and tissues were collected and examined by a certified pathologist following hematoxylin & eosin (H&E) staining.

Animal models of cholestasis

Experiments were performed in age-matched male mice on C57BL/6J genetic background (BDL mouse model)(19) at the Biodonostia Health Research Institute (BHRI) and at Syngene International Ltd. (Bangalore, India) (pharmacokinetic profile) and on *Abcb4*^{tm1Bor} genetic background (*Mdr2*$^{-/-}$ mouse)(20,21) at Gubra (Hoersholm, Denmark). Extended information provided in Supplementary Material http://links.lww.com/HEP/F6.

ACCEPTED

Liver histology

For *Mdr2*$^{-/-}$ mice, livers were fixed overnight in 4% paraformaldehyde, paraffin-embedded and sectioned (3 μm thickness). Tissue slides were stained with H&E or used for immunohistochemistry staining.

In the BDL mouse study, liver histology analysis and scoring were conducted as previously described.(19) Briefly, formalin-fixed and paraffin-embedded (FFPE) slides were stained with H&E (MERCK) for the analysis of tissue morphology. Further details are included in Supplementary Material http://links.lww.com/HEP/F6.

Downloaded from http://journals.lww.com/hep by BhDMf5ePHKav1zEoum1tQfN4a+kJLhEZgbsIHo4XMi0hCywCX1AWnYQp/IlQrHD3i3D0OdRyi7TvSFl4Cf3VC4/OAVpDDa8K2+Ya6H515kE= on 04/04/2023

Serum, plasma and liver biochemistry

Blood was collected from the tail vein (*Mdr2*$^{-/-}$ mice) or by cardiac puncture (BDL mice) for biochemical analysis. For liver biochemistry, whole liver was dissected and weighed, and a biopsy (~200 mg, less than 0.7 x 0.5 cm) was resected from the left lateral lobe. Detailed information of the methodology is provided in Supplementary Material http://links.lww.com/HEP/F6.

Bile acid and C4 analysis

BAs, and their intermediate/precursor 7α-hydroxy-4-cholesten-3-one (C4), were determined in plasma by LC-MS/MS as previously described.(22–24) In C57BL/6N wild-type (WT) mouse experiments, total BA levels were analysed in serum (Cell Biolabs), stools (Cell Biolabs) and urine (Biovision) using commercial kits following manufacturer's instructions. Further details are provided in Supplementary Material http://links.lww.com/HEP/F6.

Cholangiocyte functional studies (apoptosis by flow cytometry)

Normal rat cholangiocytes (NRC) were isolated from liver tissue of Wistar rats (Charles River Laboratories) at the BHRI (San Sebastian, Spain), and then cultured and

ACCEPTED

characterized as we previously described.(25) Cell apoptosis *in vitro* was assessed by flow cytometry as described in Supplementary Material http://links.lww.com/HEP/F6.

Downloaded from http://journals.lww.com/hep by BhDMf5ePHKav1zEoum1tQfN4a+kJLhEZgbsIHo4XMi0hCywCX1AWnYQp/IlQrHD3i3D0OdRyi7TvSFl4Cf3VC4/OAVpDDa8K2+Ya6H515kE= on 04/04/2023

Immunoblotting

Analysis of ASBT expression in NRC was performed as described in Supplementary Material http://links.lww.com/HEP/F6.

RNA isolation and quantitative real-time polymerase chain reaction (RT-qPCR)

RNA was extracted from mouse liver and ileum tissues using the Maxwell® RSC Instrument (Promega) following the manufacturer's instructions and subjected to reverse transcription followed by RT-qPCR analysis in a CFX384 Touch Real-Time PCR Detection System (BioRad). Details are outlined in Supplementary Material http://links.lww.com/HEP/F6.

RNAseq analysis

RNA sequencing (RNAseq) was performed on RNA extracts from terminal liver samples (15 mg fresh tissue), as described in detail elsewhere.(26) Untreated WT mice for analysis of *Mdr2*$^{-/-}$ mouse data as control correspond to stock liver samples from age-matched mice at Gubra. Additional details are provided in Supplementary Material http://links.lww.com/HEP/F6.

Safety, tolerability, pharmacokinetics and pharmacodynamic studies in healthy subjects

This Phase 1 study (Protocol Reference Number: A3907-001, Covance Study Number: 8445784, EudraCT Number: 2020-004423-17) was sponsored and designed by Albireo

ACCEPTED

Downloaded from http://journals.lww.com/hep by BhDMf5ePHKav1zEoum1tQfN4a+kJLhEZgbsIHo4XMi0hCywCX1AWnYQp/IlQrHD3i3D0OdRyi7TvSFl4Cf3VC4/OAVpDDa8K2+Ya6H515kE= on 04/04/2023

AB, Sweden, and conducted in accordance with both the Declarations of Helsinki and Istanbul and approved by the North-East - York Research Ethics Committee (Newcastle-upon-Tyne, UK). Informed consent was given in writing by all subjects. The study was conducted at a single site in the United Kingdom (Principal Investigator: Ashley Brooks, MB ChB, Associate Medical Director, Labcorp Clinical Research Unit Ltd., UK). Besides standard safety parameters, additional pharmacodynamic analyses included LDLc, serum BAs (total and individual), plasma C4 and FGF-19 and urine BAs. See Supplementary Material http://links.lww.com/HEP/F6 for further information.

Statistical analysis

GraphPad Prism 8 (GraphPad Software) was used to perform the statistical analysis. Normality of the data set was assessed by Shapiro-Wilk test. For comparisons of two independent groups, parametric Student's *t*-test or non-parametric Mann Whitney test were employed. When more than two related groups were compared, parametric one-way analysis of variance (ANOVA) with Dunnett's post hoc test or non-parametric Kruskal-Wallis test followed by Dunn's multiple comparison test were used. For statistical analysis of the time-course data, two-way ANOVA with Tukey's multiple comparisons post hoc test was applied. Gene set analysis was conducted with the R package PIANO version 1.18.1 using the Stouffer method, and p-values were corrected for multiple testing using the Benjamini-Hochberg method (False Discovery Rate, $p<0.05$). Data in bar graphs are expressed as mean ± standard error of the mean (SEM). Significance was defined as $p<0.05$.

Results

ACCEPTED

Downloaded from http://journals.lww.com/hep by BhDMf5ePHKav1zEoum1tQfN4a+kJLhEZgbsIHo4XMi0hCywCX1AWnYQp/IlQrHD3i3D0OdRyi7TvSFl4Cf3VC4/OAVpDDa8K2+Ya6H515kE= on 04/04/2023

ACCEPTED

A3907 is a potent, selective and orally available ASBT inhibitor that distributes to the intestine, liver and kidneys in rodents

A3907 is a potent and selective inhibitor of both mouse and human ASBT, with similar potency and selectivity as the gut-restricted ASBT inhibitor A3309(18) (Fig. 1A). Oral administration of A3907 (10 mg/kg) to rodents resulted in high exposure in plasma (Supplementary Fig S1A http://links.lww.com/HEP/F6). A3907 pharmacokinetic parameters in different species, when dosed with 10 mg/kg, were: C_{max} 558-655 (ng/ml), T_{max} 2.67-5.33 (h), AUC_{inf} 4300-8250 (h*ng/ml), 30-60% oral bioavailability and $t_{1/2}$ 4.49-7.4 (h). Moreover, oral administration of incrementing doses of A3907 (3, 10, and 30 mg/kg) in mice demonstrated a dose-dependent increase of compound concentrations in feces, serum, bile, as well as kidneys and liver, whereas low levels of A3907 were present in urine and detected only at the highest dose (Supplementary Fig S1B http://links.lww.com/HEP/F6).

QWBA analysis in rats orally administered with [^{14}C]-A3907 revealed distribution to the intestine, liver and kidney which are the main ASBT-expressing organs. By contrast, independent QWBA experiments performed with [^{14}C]-A3309 confirmed preferential accumulation to the intestine, with only trace amounts found in the liver and kidney (Figure 1B). Daily oral administration of up to 1000 mg/kg/day of A3907 to rats was well tolerated and no adverse A3907-related findings were observed after the 13-week treatment period (Supplementary Fig S1C http://links.lww.com/HEP/F6).

The pharmacodynamic profile of A3907 and A3309 was compared in normal mice. Both compounds were administered orally to non-fasted mice once daily for 7 days (3 and 10 mg/kg/day). Similar inhibition of ileal ASBT was observed for both compounds, resulting in significant elevation of fecal BA levels, while urine BA levels

did not change in response to A3907 or A3309 (Fig. 1C). As expected, ASBT inhibition led to transcriptional *Fgf15* repression in the ileum and subsequent hepatic upregulation of *Cyp7A1*, particularly evident in A3907-exposed mice, yielding increased circulating C4 levels (reflecting BA synthesis) compared to controls (Fig. 1C and D). As a result, serum BA levels in normal non-cholestatic mice remained fairly constant in all experimental groups (Fig. 1C).

A3907 reduces liver injury and markers of cholestasis in Mdr2$^{-/-}$ mice

The potential therapeutic effect of A3907 was investigated in *Mdr2*$^{-/-}$ mice, which are characterized by spontaneous and progressive development of cholestasis and sclerosing cholangitis.(20,21) *Mdr2*$^{-/-}$ mice were treated with different doses of A3907 (1, 3, 10, 30 mg/kg) once a day by oral gavage for 4 weeks (Fig. 2A).

A dose-dependent increase in A3907 levels was found in the plasma of *Mdr2*$^{-/-}$ mice, with mean values of 17, 34, 97 and 405 ng/ml, respectively, measured 2 h post-dosing (Fig. 2B). A3907 did not affect mice body weight, but dose-dependently decreased the liver-to-body and spleen-to-body weight ratios compared to vehicle controls (Fig. 2C). A3907 dose-dependently reduced plasma biomarkers of liver injury (ALT, AST) and cholestasis (ALP) (Fig. 2D). Similarly, the plasma markers of sclerosing cholangitis (*i.e.*, biliary injury and fibrosis, TIMP-1(27) and MMP-7(28)) were decreased in animals treated with A3907 compared to vehicle controls (Fig. 2D). A3907 dose-dependently decreased histological markers of ductular reaction (CK7), portal inflammation (H&E and galectin-3) and fibrogenesis (□-SMA) compared to controls (Fig. 2E). Additionally, whole liver tissue levels of the pro-inflammatory chemokine MCP-1 and the fibrosis marker hydroxyproline were also lower in A3907-treated *Mdr2*$^{-/-}$ mice compared to vehicle controls (Fig. 2F). Furthermore, A3907

Downloaded from http://journals.lww.com/hep by BhDMf5ePHKav1zEoum1tQfN4a+kJLhEZgbsIHo4XMi0hCywCX1AWnYQp/IlQrHD3i3D0OdRyi7TvSFl4Cf3VC4/OAVpDDa8K2+Ya6H515kE= on 04/04/2023

ACCEPTED

markedly reduced serum total BA levels at all doses investigated, whereas no significant changes in urinary BA and serum C4 concentrations were observed (Fig. 2F; Supplementary Fig. S2 and S3 http://links.lww.com/HEP/F6). As observed in normal mice, A3907 treatment led to ileal *Fgf15* downregulation and consequent *Cyp7a1* upregulation in the liver (Supplementary Fig. S4 http://links.lww.com/HEP/F6).

Collectively, our data indicate that A3907 protects *Mdr2*$^{-/-}$ mice from BA-induced ductular reaction and liver injury. The fact that all doses of A3907 similarly reduced serum BA levels, while the effects on ductular reaction were progressively and dose-dependently improved suggests that normalizing BA load (which can often be achieved with intestinally restricted ASBT inhibitors) is not the only contributing factor to the improved ductular/liver protection. This may point towards direct target engagement of ASBT on cholangiocytes as a potential additive effect of A3907.

A3907 prevents BA-induced cholangiocyte apoptosis in vitro

Expression of ASBT in cultured cholangiocytes was confirmed by immunoblotting in normal rat cholangiocytes (NRCs) (Supplementary Fig. S5 http://links.lww.com/HEP/F6). In order to mimic a context of cholestasis and sclerosing cholangitis, cholangiocytes were incubated with toxic concentrations of GCDCA (1 mM) *in vitro*. Flow cytometry experiments indicated that co-incubation of cholangiocytes with A3907 prevented BA-induced apoptosis. By contrast, and as expected, the apoptotic effect of the antibiotic puromycin (non-ASBT substrate) on cholangiocytes was not affected by A3907 exposure (Fig. 3A).

A3907 normalizes hepatic gene signatures of inflammation, regeneration, damage and fibrosis in Mdr2$^{-/-}$ mice

Downloaded from http://journals.lww.com/hep by BhDMf5ePHKav1zEoum1tQfN4a+kJLhEZgbsIHo4XMi0hCywCX1AWnYQp/IlQrHD3i3D0OdRyi7TvSFl4Cf3VC4/OAVpDDa8K2+Ya6H515kE= on 04/04/2023

ACCEPTED

Downloaded from http://journals.lww.com/hep by BhDMf5ePHKav1zEoum1tQfN4a+kJLhEZgbsIHo4XMi0hCywCX1AWnYQp/IlQrHD3i3D0OdRyi7TvSFl4Cf3VC4/OAVpDDa8K2+Ya6H515kE= on 04/04/2023

RNAseq analysis of liver samples from *Mdr2*$^{-/-}$ mice revealed important biological processes modulated by A3907. Vehicle-dosed *Mdr2*$^{-/-}$ mice displayed marked perturbations in the liver transcriptome as indicated by an excessive number of differentially expressed genes (DEGs, n=9,047) compared to WT mice. Among them, the levels of 443 DEGs were normalized in *Mdr2*$^{-/-}$ mice treated with 3 mg/kg/day A3907 (108 upregulated and 335 downregulated following A3907 treatment; Fig. 3B). Gene ontology (GO) enrichment analysis of these 443 DEGs normalized by A3907 revealed the influence of this compound on several important biological processes, including fibrosis, inflammation, cell proliferation and apoptosis, endoplasmic reticulum stress and steroid metabolism (Fig. 3C-D; Supplementary Fig. S6 http://links.lww.com/HEP/F6). Of note, the increased expression levels of *S1pr2* observed in *Mdr2*$^{-/-}$ mice, a receptor closely related to cholangiocyte proliferation and cholestatic injury in response to conjugated BAs,(29) were reduced by A3907 (Fig. 3E).

A3907 enhances renal BA clearance and halts liver disease progression in experimental obstructive cholestasis

Proximal *tubuli* epithelial cells lining the urinary tract represent another cell target for A3907. Here, apical ASBT reclaims renally filtered BAs.(9) While our data in *Mdr2*$^{-/-}$ mice suggests that inhibition of intestinal and biliary ASBT could be sufficient to reverse increased plasma BA levels, we investigated whether renal ASBT inhibition could be a novel mechanism to ameliorate cholestasis during biliary obstructive conditions. Thus, we evaluated the efficacy of A3907 in a model of obstructive cholestasis (BDL mice), where entero-hepatic circulation of BAs is blocked and BAs can therefore only be excreted *via* renal clearance. We also used locally-acting A3309 as a comparator.

ACCEPTED

Downloaded from http://journals.lww.com/hep by BhDMf5ePHKav1zEoum1tQfN4a+kJLhEZgbsIHo4XMi0hCywCX1AWnYQp/IlQrHD3i3D0OdRyi7TvSFl4Cf3VC4/OAVpDDa8K2+Ya6H515kE= on 04/04/2023

Three days after surgery, BDL mice were treated with different daily doses of A3907 (3, 10, 30 mg/kg) or A3309 (3 mg/kg) by oral gavage for 11 days (Fig. 4A). Twenty-four h after the last A3907 administration, a dose-dependent increase in A3907 levels was observed in serum (mean values of 34, 48 and 197 ng/ml, respectively) and in bile (mean values of 75, 251 and 1358 ng/ml, respectively) (Fig. 4B), suggesting that A3907 reaches ASBT on the apical surface of cholangiocytes at pharmacologically relevant concentrations. BDL mice receiving vehicle demonstrated pronounced body weight loss, as compared to sham-operated control mice, and this progressive body weight loss was reversed by all A3907 doses (Fig. 4C). Liver histopathological analyses indicated lower hepatic inflammatory cell infiltration and fewer necrotic areas in A3907-treated BDL mice compared to vehicle (Fig. 4D). A3907 markedly enhanced the excretion of urinary BAs, predominantly the hydrophilic TMCAs and TCA, by up to 90-fold, compared to vehicle controls (Fig. 4E; Supplementary Fig S7 http://links.lww.com/HEP/F6). This led to reduced serum and bile levels of total BAs compared to control BDL mice. In agreement, an inverse correlation between serum *vs* urine BA levels was observed in BDL mice (Fig. 4E). As observed for *Mdr2*$^{-/-}$ mice, no changes in serum C4 concentrations were found in the A3907-treated BDL mice (Supplementary Fig. S3 http://links.lww.com/HEP/F6). Compared to vehicle, A3907 also reduced BDL-induced increases in serum levels of transaminases (AST and ALT), bilirubin (total, direct and indirect) and urea, as well as total and LDL cholesterol, while counteracting the decreased serum levels of albumin, HDL and glucose (Fig. 4F). In contrast, ALP levels remained unchanged following A3907 treatment (Fig 4F).

Altogether, these results suggest that experimental obstructive cholestasis can be ameliorated by A3907-induced ASBT inhibition in the kidneys, enhancing renal BA clearance to reduce the BA load and liver toxicity and improving liver health.

ACCEPTED

Downloaded from http://journals.lww.com/hep by BhDMf5ePHKav1zEoum1tQfN4a+kJLhEZgbsIHo4XMi0hCywCX1AWnYQp/IlQrHD3i3D0OdRyi7TvSFl4Cf3VC4/OAVpDDa8K2+Ya6H515kE= on 04/04/2023

Next, we compared the pharmacokinetic and therapeutic effects of A3907 with the intestinally-restricted ASBTi A3309 in the BDL model. For that purpose, we first characterized the systemic exposure of both compounds in BDL mice orally administered with daily doses of each compound (3 or 10 mg/kg) for 7 days (Fig. 5A). As expected, A3907 displayed high systemic bioavailability, reaching mean serum concentration peaks of 193 and 936 ng/ml in BDL mice treated once daily with 3 or 10 mg/kg, respectively (Fig. 5A). Interestingly, A3309 was also detected in serum of the BDL mice after 7 days of treatment. These plasma exposures were approximately 6-fold higher than exposures reached in normal WT mice under the same experimental conditions (data not shown). This discrepancy is probably explained by a general increase in intestinal permeability in response to the BDL procedure. However, serum levels of A3309 were significantly lower than A3907 (Fig. 5A). In this regard, although both compounds induced urinary BA excretion to some extent, only A3907 was able to significantly reduce both serum and biliary BAs levels in BDL mice, while A3309 attenuated BA levels in a non-significant fashion (Fig. 5B). By contrast, no changes in fecal BA content were observed in any of the experimental groups (Supplementary Figure S8 http://links.lww.com/HEP/F6). The superior efficacy of A3907 in relieving BA overload was mirrored by its capacity to prevent BDL-associated progressive body weight loss as well as to reduce the exacerbated levels of transaminases and urea in the BDL mice (Fig. 5C-D). Hence, the mild effects of A3309 together with its lower but still present systemic bioavailability, seem to reinforce the importance of systemic ASBTi in a biliary obstructive context.

A3907 normalizes the dysregulated transcriptional profile of BDL mouse livers

ACCEPTED

Downloaded from http://journals.lww.com/hep by BhDMf5ePHKav1zEoum1tQfN4a+kJLhEZgbsIHo4XMi0hCywCX1AWnYQp/IlQrHD3i3D0OdRyi7TvSFl4Cf3VC4/OAVpDDa8K2+Ya6H515kE= on 04/04/2023

ACCEPTED

Similar to observations in *Mdr2*$^{-/-}$ mice, transcriptomic analysis of liver samples from BDL mice revealed substantial perturbations in hepatic global gene expression (5,790 DEGs) compared to sham-operated control mice. A3907 (3 mg/kg/day) normalized the expression of 303 dysregulated genes (126 upregulated and 177 downregulated following A3907 treatment) in BDL mice (Fig. 6A), while only 15 genes were normalized by A3309 (3 mg/kg/day). GO enrichment analysis of genes normalized by A3907 revealed genes participating in important processes related to BA and liver homeostasis, as well as to cell growth, oxidative stress, lipid metabolism and homeostasis, cell transport, xenobiotic metabolism, coenzyme metabolism and TOR signaling (Fig. 6B-C). Increased expression levels of the genes encoding for the nuclear receptor PXR and the basolateral transporter OST-β mice (proteins involved in hepatocyte basolateral BA efflux)(30) were found upregulated in BDL mice, compared to sham, and were specifically normalized following A3907 treatment (Fig. 6D).

Phase 1 study of A3907 safety, tolerability, oral bioavailability and pharmacodynamic effects in healthy humans

Considering the positive preclinical effects of A3907 in experimental models of cholestatic liver disease, we investigated the tolerability, pharmacokinetics and pharmacodynamic effects of A3907 in healthy human subjects in a single-ascending-dose study (SAD) (data not shown), followed by a multiple-ascending-dose (MAD) study (Fig. 7A). The SAD study revealed that A3907 exposure increased proportionally to doses from 1 to 81 mg. The MAD clinical trial indicated that daily oral administration of A3907 for 7 days was well-tolerated in the dose range investigated (9, 27 and 67.5 mg), showing no serious treatment-emergent adverse events (TEAEs) (Supplementary Table S4 http://links.lww.com/HEP/F6). The most frequent adverse

effects were mild, *i.e.*, diarrhea and headache. Oral administration of 67.5 mg A3907 resulted in significant compound exposure in plasma (Fig. 7B), with a C_{max} of 78.3 ng/ml, a T_{max} of 8 h, an AUC_{inf} of 810 h*ng/ml and a $t_{1/2}$ of 8.4 h (Fig. 7B). A similar pharmacokinetic profile was obtained on days 1 and 7 after daily oral administration (Supplementary Table S5 http://links.lww.com/HEP/F6).

Functionally, A3907 significantly decreased postprandial plasma total BA levels relative to baseline in healthy humans (Fig. 7C). While levels of un-conjugated BAs (CA, LCA, DCA, CDCA, UDCA) remained unaltered, A3907 significantly decreased the postprandial rise in plasma levels of conjugated BAs (GCA, GLCA, GDCA, GCDCA, GUDCA, TCA, TLCA, TDCA, TCDCA, TUDCA) as compared to baseline (Fig. 7C). Similar to normal mice, BAs were gradually normalized in healthy human subjects administered A3907 potentially due to compensatory increases in liver BA synthesis as indicated by increased circulating C4 levels, compared to controls (Fig. 7C). Importantly, plasma exposure of A3907 in healthy subjects was within the range of plasma concentrations that achieved anti-cholestatic efficacy in *Mdr2*$^{-/-}$ and BDL mice (Fig 7D), supporting potential translation to human cholestatic liver disease. By contrast, the systemic A3309 exposure observed in humans at the therapeutically relevant dose was several-fold lower than levels demonstrating signs of efficacy in BDL mice in the current study (Fig. 7D). This questions the human translational relevance of the preclinical findings with A3309 presented in the current study.

Discussion

Previous preclinical and clinical studies have demonstrated that locally-acting intestinal ASBTis are effective in reducing BA load. For instance, SC-435(31) and A4250 (odevixibat)(32) reduced BA levels in serum and bile, and improved cholestatic liver

Downloaded from http://journals.lww.com/hep by BhDMf5ePHKav1zEoum1tQfN4a+kJLhEZgbsIHo4XMi0hCywCX1AWnYQp/IlQrHD3i3D0OdRyi7TvSFl4Cf3VC4/OAVpDDa8K2+Ya6H515kE= on 04/04/2023

ACCEPTED

Downloaded from http://journals.lww.com/hep by BhDMf5ePHKav1zEoum1tQfN4a+kJLhEZgbsIHo4XMi0hCywCX1AWnYQp/IlQrHD3i3D0OdRyi7TvSFl4Cf3VC4/OAVpDDa8K2+Ya6H515kE= on 04/04/2023

disease in *Mdr2*$^{-/-}$ mice. Clinically, odevixibat and maralixibat reduced BA load and decreased pruritus in pediatric indications such as progressive familial intrahepatic cholestasis(16) and Alagille syndrome(12), respectively. However, while locally-acting ASBTis effectively reduced BA load and pruritus in adult cholestatic cholangiopathies such as PBC and PSC, they did not have a meaningful impact on biomarkers believed to reflect disease progression such as ALP or ALT/AST and were often associated with dose-limiting diarrhea.(33–35) Furthermore, since the therapeutic outcome of intestinal ASBTis relies on intestinal inhibition of BA reabsorption, the efficacy of these drugs is likely limited in cholestatic situations where the bile flow is severely compromised, such as obstructive cholestasis. In the current study we report: *i*) the discovery and characterization of A3907, the first oral systemically-available ASBTi in clinical development, *ii*) its multi-modal effects on BA reabsorption and signaling in cholangitis (*Mdr2*$^{-/-}$ mouse) and obstructive cholestasis (BDL) mouse models, *iii*) a detailed assessment of its translational potential to humans, and *iv*) a summary of its tolerability, pharmacokinetics and pharmacodynamics in healthy subjects.

In WT mice, oral A3907 distributed to key ASBT-expressing organs such as ileum, liver and kidney. Also, A3907 stimulated fecal excretion of BAs without affecting urinary BA levels, being in agreement with fecal BA excretion as the main route for eliminating BAs under physiological conditions.(36) As expected, this effect was rapidly counterbalanced by intestinal *Fgf15* reduction and subsequent increased BA synthesis, underscoring the tightly controlled BA homeostasis under normal conditions. As for normal mice, high systemic A3907 exposure was confirmed in both *Mdr2*$^{-/-}$ and BDL mice.

Liver injury in *Mdr2*$^{-/-}$ mice is caused by loss of canalicular biliary phospholipid secretion resulting in excessive biliary accumulation of free BAs, that leads to

ACCEPTED

Downloaded from http://journals.lww.com/hep by BhDMf5ePHKav1zEoum1tQfN4a+kJLhEZgbsIHo4XMi0hCywCX1AWnYQp/IlQrHD3i3D0OdRyi7TvSFl4Cf3VC4/OAVpDDa8K2+Ya6H515kE= on 04/04/2023

cholangiocyte injury, pericholangitis, periductal fibrosis with ductular proliferation and eventually progression to sclerosing cholangitis.(20,21) A3907 dose-dependently reduced liver- and spleen-to-body weight ratios, plasma markers of liver injury, as well as improved several liver histological markers of inflammation and ductular reaction in *Mdr2*$^{-/-}$ mice. It is noteworthy that A3907 significantly lowered hepatic α-SMA levels, a reliable marker of fibrogenic stellate cell activation,(37,38) in addition to reduced plasma and liver biochemical markers of fibrosis. Moreover, RNAseq analysis of livers revealed that A3907 impacted important biological processes related to cholestatic liver injury, for instance normalizing the expression of key related genes like *S1pr2*, which is closely related to cholangiocyte proliferation and cholestatic injury in response to conjugated BAs. Interestingly, in *Mdr2*$^{-/-}$ mice, the lowest dose of A3907 tested (1 mg/kg/day) was sufficient to induce maximal serum BA reduction. However, higher doses of A3907 provided additional dose-dependent anti-cholestatic, anti-inflammatory and anti-fibrogenic effects, suggesting that A3907 can also provide additional beneficial effects independent from its ability to decrease systemic BA overload. In this regard, targeting ASBT at the site of insult (cholangiocytes *per se*) and subsequent inhibition of local BA transport and ASBT-mediated signaling may contribute to the additional efficacy observed for A3907. In line with this, the high levels of A3907 found in bile, together with its capacity to attenuate cytotoxic effects of hydrophobic BAs in cultured cholangiocytes provide support for the cholangiocyte-protective effect of A3907.

The robust hepatoprotective effects of A3907 were corroborated in BDL mice, a model of obstructive cholestasis where the entero-hepatic circulation of BAs is blocked. A3907 evoked profound urinary excretion of BAs in BDL mice. We estimated that the urinary excretion of BAs following A3907 administration to BDL mice may reach levels of up to 10 µmol/day, which is reflected by reductions in serum and biliary BA

ACCEPTED

Downloaded from http://journals.lww.com/hep by BhDMf5ePHKav1zEoum1tQfN4a+kJLhEZgbsIHo4XMi0hCywCX1AWnYQp/IlQrHD3i3D0OdRyi7TvSFl4Cf3VC4/OAVpDDa8K2+Ya6H515kE= on 04/04/2023

ACCEPTED

levels. As a result of the marked renal clearance of BAs, hallmarks of severe progressive cholestatic liver injury in BDL mice, including acute obstructive jaundice and hepatic necro-inflammation, were partially reversed following A3907 treatment. Furthermore, A3907 also suppressed the extreme elevations of circulating liver enzymes, BAs, total bilirubin and cholesterol in this model. These results provide strong evidence about the promising translational potential of A3907 in conditions where the bile flow is physically blocked, like situations of common bile duct stenosis or distal cholangiocarcinomas.

Interestingly, measurable concentrations of the A3309 were also detected in serum of BDL mice treated with 3 mg/kg/day dose of this compound, probably as a result of increased intestinal permeability following BDL surgery.(39) However, A3309 proved significantly less effective in relieving systemic BA overload and improving pathophysiological hallmarks of cholestatic disease. Most importantly, the systemic exposures of A3309 needed for the observed effects in the BDL mice are far from the trace levels obtained in humans at therapeutically relevant doses,(18) suggesting limited translational potential for the treatment of obstructive forms of cholestasis. Furthermore, as in *Mdr2*$^{-/-}$ mice, transcriptomic analysis showed that only A3907 was able to modulate important hepatic-dysregulated processes during obstructive cholestasis (BDL), including cell growth, oxidative stress, lipid metabolism and homeostasis, and xenobiotic metabolism, among others. All these results are further supported by a previous work demonstrating that *Asbt*$^{-/-}$ mice are partially resistant to BDL-induced liver injury, linked to increased urinary BA excretion and consequently lower systemic BA levels.(40)

Phase I studies demonstrated that A3907 is well-tolerated and shows favourable pharmacokinetics at pharmacologically active doses. Accordingly, A3907 reduced

Downloaded from http://journals.lww.com/hep by BhDMf5ePHKav1zEoum1tQfN4a+kJLhEZgbsIHo4XMi0hCywCX1AWnYQp/IlQrHD3i3D0OdRyi7TvSFl4Cf3VC4/OAVpDDa8K2+Ya6H515kE= on 04/04/2023

ACCEPTED

postprandial circulating levels of conjugated BAs and dose-dependently increased serum C4 levels, a marker of BA synthesis downstream of CYP7A1(41) in healthy human subjects (and in normal mice). Increases in circulating C4 levels are an expected compensatory response to ASBT inhibition that has been observed for most gut-restricted ASBT inhibitors in healthy humans. However, unlike other inhibitors, well-tolerated oral doses of A3907 in humans resulted in plasma levels resembling those observed at therapeutically effective doses in experimental models of cholestasis.

ASBTis have emerged as promising drugs to expand the currently limited pharmacological toolbox for the treatment of cholestasis. Both locally-acting(31,32) and systemic ASBTis have shown to improve cholestatic liver injury in *Mdr2*$^{-/-}$ mice. However, the therapeutic efficacies reported in these studies are not comparable due to methodological differences. While A3907 and A4250 were investigated in adult (8 weeks) mice and treatment was extended over 4 weeks,(32) experiments with SC-435 were conducted in younger animals (4 weeks) treated for a shorter period (2 weeks).(31) Moreover, the range of doses employed was different between studies. Therefore, future investigations including direct comparisons between locally-acting and systemic ASBTis in different experimental models of cholestasis (not only in BDL mice) will provide further insights on their therapeutic similarities and differences. Finally, the translation of preclinical results into human cholestatic situations should be interpreted with caution due to intrinsic limitations of experimental models to resemble the complex and heterogeneous scenario of human cholestatic disorders.(42,43)

In conclusion, A3907 is the first oral systemic ASBT inhibitor that acts at the level of the intestine, liver and kidney to robustly attenuate cholestatic liver damage in experimental models. Our data indicate that the unique systemic nature of A3907, compared to intestinally restricted ASBTis, represents an opportunity for the treatment

in clinical manifestations where the bile flow is physically blocked (*e.g.*, common bile duct stenosis or distal cholangiocarcinomas), providing new avenues for treatments. Furthermore, the cholangiocyte-targeting and protection capacity of A3907 may be valuable to improve outcomes for patients suffering from cholangiopathies such PBC and PSC. Importantly, the A3907 exposures achieved in healthy subjects were comparable to those required for attaining therapeutic effects in animal models of cholestasis, suggesting translational potential. Further clinical studies will be needed to determine the efficacy, safety and optimal dosing regimens of A3907 in patients with chronic cholestatic liver disease such as PBC and PSC.

Downloaded from http://journals.lww.com/hep by BhDMf5ePHKav1zEoum1tQfN4a+kJLhEZgbsIHo4XMi0hCywCX1AWnYQp/IlQrHD3i3D0OdRyi7TvSFl4Cf3VC4/OAVpDDa8K2+Ya6H515kE= on 04/04/2023

ACCEPTED

Acknowledgements

We thank Professor Paul Dawson from the Emory University School of Medicine in Atlanta for generously provide the primary antibody used to assess ASBT expression in NRC. Ms. Ingela Arvidsson and Ms. Jennifer Härdfeldt at Karolinska Institutet at Karolinska University Hospital Huddinge, Stockholm (Sweden), for skilful analyses at the mass spectrometry laboratory. Simon Evers, study director on the *Mdr2*$^{-/-}$ study and Michael Feigh, contributed to study design and interpretation of data of the *Mdr2*$^{-/-}$ study at Gubra, Denmark. Judit Bartis, Ben Kohn at Albireo for leading the manufacturing of A3907. Santosh Kulkarni, Runa Pal, Shivendra Singh, Ramesh Kangarajan and Ashwani Gaur from Syngene International Ltd., Bangalore, India, for, in collaboration with Albireo, manufacturing of the compound and *in vitro* and *in vivo* evaluation of A3907.

References

1. Banales JM, Huebert RC, Karlsen T, Strazzabosco M, LaRusso NF, Gores GJ. Cholangiocyte pathobiology. *Nat. Rev. Gastroenterol. Hepatol.* 2019;16:269–281.
2. Feldman AG, Sokol RJ. Neonatal cholestasis: emerging molecular diagnostics and potential novel therapeutics. *Nat. Rev. Gastroenterol. Hepatol. 2019 166.* 2019;16:346–360.
3. de Vries E, Beuers U. Management of cholestatic disease in 2017. *Liver Int.* 2017;37 Suppl 1:123–129.
4. De Vloo C, Nevens F. Cholestatic pruritus : an update. *Acta Gastroenterol. Belg.* 2019;82:75–82.
5. Dyson JK, Beuers U, Jones DEJ, Lohse AW, Hudson M. Primary sclerosing cholangitis. *Lancet (London, England).* 2018;391:2547–2559.
6. Yokoda RT, Carey EJ. Primary Biliary Cholangitis and Primary Sclerosing Cholangitis. *Am. J. Gastroenterol.* 2019;114:1593–1605.
7. Slijepcevic D, Van De Graaf SFJ. Bile Acid Uptake Transporters as Targets for Therapy. *Dig. Dis.* 2017;35:251–258.
8. Di Ciaula A, Garruti G, Baccetto RL, Molina-Molina E, Bonfrate L, Wang DQH, et al. Bile Acid Physiology. *Ann. Hepatol.* 2017;16:s4–s14.
9. St-Pierre M V., Kullak-Ublick GA, Hagenbuch B, Meier PJ. Transport of bile acids in hepatic and non-hepatic tissues. *J. Exp. Biol.* 2001;204:1673–1686.
10. Durník R, Šindlerová L, Babica P, Jurček O. Bile Acids Transporters of Enterohepatic Circulation for Targeted Drug Delivery. *Molecules.* 2022;27:2961.
11. Trottier J, Białek A, Caron P, Straka RJ, Heathcote J, Milkiewicz P, et al. Metabolomic profiling of 17 bile acids in serum from patients with primary biliary cirrhosis and primary sclerosing cholangitis: A pilot study. *Dig. Liver Dis.* 2012;44:303–310.
12. Gonzales E, Hardikar W, Stormon M, Baker A, Hierro L, Gliwicz D, et al. Efficacy and safety of maralixibat treatment in patients with Alagille syndrome and cholestatic pruritus (ICONIC): a randomised phase 2 study. *Lancet.* 2021;398:1581–1592.
13. Yang N, Dong YQ, Jia GX, Fan SM, Li SZ, Yang SS, et al. ASBT(SLC10A2): A promising target for treatment of diseases and drug discovery. *Biomed.*

Downloaded from http://journals.lww.com/hep by BhDMf5ePHKav1zEoum1tQfN4a+kJLhEZgbsIHo4XMi0hCywCX1AWnYQp/IlQrHD3i3D0OdRyi7TvSFl4Cf3VC4/OAVpDDa8K2+Ya6H515kE= on 04/04/2023

ACCEPTED

Downloaded from http://journals.lww.com/hep by BhDMf5ePHKav1zEoum1tQfN4a+kJLhEZgbsIHo4XMi0hCywCX1AWnYQp/IlQrHD3i3D0OdRyi7TvSFl4Cf3VC4/OAVpDDa8K2+Ya6H515kE= on 04/04/2023

Pharmacother. 2020;132:110835.

14. Al-Dury S, Marschall HU. Ileal Bile Acid Transporter Inhibition for the Treatment of Chronic Constipation, Cholestatic Pruritus, and NASH. *Front. Pharmacol.* 2018;9.
15. Graffner H, Gillberg PG, Rikner L, Marschall HU. The ileal bile acid transporter inhibitor A4250 decreases serum bile acids by interrupting the enterohepatic circulation. *Aliment. Pharmacol. Ther.* 2016;43:303–310.
16. Thompson RJ, Arnell H, Artan R, Baumann U, Calvo PL, Czubkowski P, et al. Odevixibat treatment in progressive familial intrahepatic cholestasis: a randomised, placebo-controlled, phase 3 trial. *Lancet. Gastroenterol. Hepatol.* 2022;7.
17. Gijbels E, Pieters A, De Muynck K, Vinken M, Devisscher L. Rodent models of cholestatic liver disease: A practical guide for translational research. *Liver Int.* 2021;41:656–682.
18. Wong BS, Camilleri M. Elobixibat for the treatment of constipation. *Expert Opin. Investig. Drugs.* 2013;22:277–284.
19. **Labiano I, Agirre-Lizaso A,** Olaizola P, Echebarria A, Huici-Izagirre M, Olaizola I, et al. TREM-2 plays a protective role in cholestasis by acting as a negative regulator of inflammation. *J. Hepatol.* 2022;
20. Smit JJM, Schinkel AH, Elferink RPJO, Groen AK, Wagenaar E, van Deemter L, et al. Homozygous disruption of the murine mdr2 P-glycoprotein gene leads to a complete absence of phospholipid from bile and to liver disease. *Cell.* 1993;75:451–462.
21. Fickert P, Zollner G, Fuchsbichler A, Stumptner C, Weiglein AH, Lammert F, et al. Ursodeoxycholic acid aggravates bile infarcts in bile duct-ligated and Mdr2 knockout mice via disruption of cholangioles. *Gastroenterology.* 2002;123:1238–1251.
22. Huang J, Bathena SPR, Csanaky IL, Alnouti Y. Simultaneous characterization of bile acids and their sulfate metabolites in mouse liver, plasma, bile, and urine using LC-MS/MS. *J. Pharm. Biomed. Anal.* 2011;55:1111–1119.
23. Al-Khaifi A, Straniero S, Voronova V, Chernikova D, Sokolov V, Kumar C, et al. Asynchronous rhythms of circulating conjugated and unconjugated bile acids in the modulation of human metabolism. *J. Intern. Med.* 2018;284:546–559.
24. Straniero S, Laskar A, Savva C, Härdfeldt J, Angelin B, Rudling M. Of mice and

ACCEPTED

Downloaded from http://journals.lww.com/hep by BhDMf5ePHKav1zEoum1tQfN4a+kJLhEZgbsIHo4XMi0hCywCX1AWnYQp/IlQrHD3i3D0OdRyi7TvSFl4Cf3VC4/OAVpDDa8K2+Ya6H515kE= on 04/04/2023

men: murine bile acids explain species differences in the regulation of bile acid and cholesterol metabolism. *J. Lipid Res.* 2020;61:480–491.

25. Banales JM, Arenas F, Rodríguez-Ortigosa CM, Sáez E, Uriarte I, Doctor RB, et al. Bicarbonate-rich choleresis induced by secretin in normal rat is taurocholate-dependent and involves AE2 anion exchanger. *Hepatology.* 2006;43:266–275.
26. Hansen HH, Ægidius HM, Oró D, Evers SS, Heebøll S, Eriksen PL, et al. Human translatability of the GAN diet-induced obese mouse model of non-alcoholic steatohepatitis. *BMC Gastroenterol.* 2020;20.
27. Ueno T, Tamaki S, Sugawara H, Inuzuka S, Torimura T, Sata M, et al. Significance of serum tissue inhibitor of metalloproteinases-1 in various liver diseases. *J. Hepatol.* 1996;24:177–184.
28. Lam S, Singh R, Dillman JR, Trout AT, Serai SD, Sharma D, et al. Serum Matrix Metalloproteinase 7 Is a Diagnostic Biomarker of Biliary Injury and Fibrosis in Pediatric Autoimmune Liver Disease. *Hepatol. Commun.* 2020;4:1680–1693.
29. **Wang Y, Aoki H, Yang J,** Peng K, Liu R, Li X, et al. The role of sphingosine 1-phosphate receptor 2 in bile-acid-induced cholangiocyte proliferation and cholestasis-induced liver injury in mice. *Hepatology.* 2017;65:2005–2018.
30. Halilbasic E, Claudel T, Trauner M. Bile acid transporters and regulatory nuclear receptors in the liver and beyond. *J. Hepatol.* 2013;58:155–168.
31. Miethke AG, Zhang W, Simmons J, Taylor AE, Shi T, Shanmukhappa SK, et al. Pharmacological inhibition of apical sodium-dependent bile acid transporter changes bile composition and blocks progression of sclerosing cholangitis in multidrug resistance 2 knockout mice. *Hepatology.* 2016;63:512–523.
32. **Baghdasaryan A, Fuchs CD,** Österreicher CH, Lemberger UJ, Halilbasic E, Påhlman I, et al. Inhibition of intestinal bile acid absorption improves cholestatic liver and bile duct injury in a mouse model of sclerosing cholangitis. *J. Hepatol.* 2016;64:674–681.
33. **Hegade VS, Kendrick SFW,** Dobbins RL, Miller SR, Thompson D, Richards D, et al. Effect of ileal bile acid transporter inhibitor GSK2330672 on pruritus in primary biliary cholangitis: a double-blind, randomised, placebo-controlled, crossover, phase 2a study. *Lancet (London, England).* 2017;389:1114–1123.
34. Mayo MJ, Pockros PJ, Jones D, Bowlus CL, Levy C, Patanwala I, et al. A Randomized, Controlled, Phase 2 Study of Maralixibat in the Treatment of Itching Associated With Primary Biliary Cholangitis. *Hepatol. Commun.*

ACCEPTED

Downloaded from http://journals.lww.com/hep by BhDMf5ePHKav1zEoum1tQfN4a+kJLhEZgbsIHo4XMi0hCywCX1AWnYQp/IlQrHD3i3D0OdRyi7TvSFl4Cf3VC4/OAVpDDa8K2+Ya6H515kE= on 04/04/2023

2019;3:365–381.

35. **Levy C, Kendrick S,** Bowlus CL, Tanaka A, Jones D, Kremer AE, et al. GLIMMER: A Randomized Phase 2b Dose-Ranging Trial of Linerixibat in Primary Biliary Cholangitis Patients With Pruritus. *Clin. Gastroenterol. Hepatol.* 2022;
36. Hofmann AF. Biliary secretion and excretion in health and disease: Current concepts. *Ann. Hepatol.* 2007;6:15–27.
37. Nouchi T, Tanaka Y, Tsukada T, Sato C, Marumo F. Appearance of alpha-smooth-muscle-actin-positive cells in hepatic fibrosis. *Liver.* 1991;11:100–105.
38. Carpino G, Morini S, Ginanni Corradini S, Franchitto A, Merli M, Siciliano M, et al. Alpha-SMA expression in hepatic stellate cells and quantitative analysis of hepatic fibrosis in cirrhosis and in recurrent chronic hepatitis after liver transplantation. *Dig. Liver Dis.* 2005;37:349–356.
39. Cabrera-Rubio R, Patterson AM, Cotter PD, Beraza N. Cholestasis induced by bile duct ligation promotes changes in the intestinal microbiome in mice. *Sci. Rep.* 2019;9.
40. Kunst RF, Waart DR de, Wolters F, Duijst S, Vogels EW, Bolt I, et al. Systemic ASBT inactivation protects against liver damage in obstructive cholestasis in mice. *JHEP Reports.* 2022;0:100573.
41. Sauter G, Berr F, Beuers U, Fischer S, Paumgartner G. Serum concentrations of 7alpha-hydroxy-4-cholesten-3-one reflect bile acid synthesis in humans. *Hepatology.* 1996;24:123–126.
42. Fickert P. Time to say goodbye to the drug or the model? - why do drugs fail to live up to their promise in bile duct ligated mice? *J. Hepatol.* 2014;60:12–15.
43. **Fickert P, Pollheimer MJ,** Beuers U, Lackner C, Hirschfield G, Housset C, et al. Characterization of animal models for primary sclerosing cholangitis (PSC). *J. Hepatol.* 2014;60:1290–1303.

Figure 1. Activity, selectivity, biodistribution and pharmacodynamics of A3907 and A3309 in healthy rodents. (**A**) Human or mouse ASBT and NTCP transporters were independently overexpressed in CHOK1 cells. A3907 was tested at 10 different

ACCEPTED

concentrations to calculate the average IC_{50} value for each transporter. (**B**) Representative images of whole-body autoradiogram 4 h after a single oral administration of [^{14}C]-A3907 (10 MBq/kg) or [^{14}C]-A3309 (7.8 MBq/kg) to male rats (separate experiments), enlarged autoradiogram section of the kidney (black or red/pink regions represent areas with higher concentrations of radioactivity), and quantitative analysis of the concentration of each compound in different tissues. bld, below limit of detection. (**C**) Fecal BA concentrations in feces collected between day 6 and 7 of treatment, time profile of serum BA and C4 concentrations in C57BL/6N mice after 7 days of daily oral treatment (samples collected at 0, 2, 4, 8 and 24 h after compound administration), and urinary BA concentrations 2 h post-dose on day 8 (terminal). (**D**) Ileal *Fgf15* and hepatic *Cyp7a1* expressions measured by RT-qPCR in C57BL/6NTac mice exposed to daily oral doses of A3907, A3309 or vehicle. All statistical data represents comparison *vs* vehicle group. For statistical analysis of fecal or urine BA concentrations, parametric one-way ANOVA with Dunnett's post hoc test was used. For statistical analysis of RT-qPCR data, student´s t-test or Mann-Whitney test was applied depending on the distribution of the data. Statistical significance of serum C4 and BA concentrations overtime was assessed by two-way ANOVA with Tukey's multiple comparisons post hoc test. *p<0.05; **p<0.01 and ***p<0.001.

Downloaded from http://journals.lww.com/hep by BhDMf5ePHKav1zEoum1tQfN4a+kJLhEZgbsIHo4XMi0hCywCX1AWnYQp/IlQrHD3i3D0OdRyi7TvSFl4Cf3VC4/OAVpDDa8K2+Ya6H515kE= on 04/04/2023

ACCEPTED

Downloaded from http://journals.lww.com/hep by BhDMf5ePHKav1zEoum1tQfN4a+kJLhEZgbsIHo4XMi0hCywCX1AWnYQp/IlQrHD3i3D0OdRyi7TvSFl4Cf3VC4/OAVpDDa8K2+Ya6H515kE= on 04/04/2023

ACCEPTED

Figure 1

A

	ACTIVITY & SELECTIVITY (*in vitro*)			
	Species	**ASBT IC_{50} (nM)**	**NTCP IC_{50} (nM)**	**NTCP/ASBT ratio (IC_{50})**
A3907	Mouse	3.2	3423	1082
	Human	5.3	2796	532

B

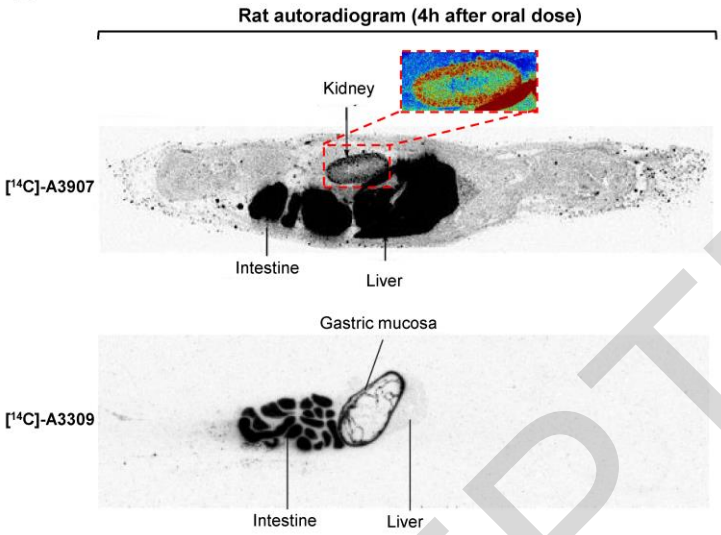

(nmol/g)	A3907	A3309
Adrenal	2.06	bld
Brain	0.02	—
Epididymis	0.18	—
Liver	76.51	0.058
Kidney-cortex	1.58	0.041
Kidney-medulla	1.12	bld
Skeletal muscle	0.56	bld
Lung	1.29	bld
Skin	0.78	bld
Small intestine	76.25	45
Spleen	1.36	bld

C

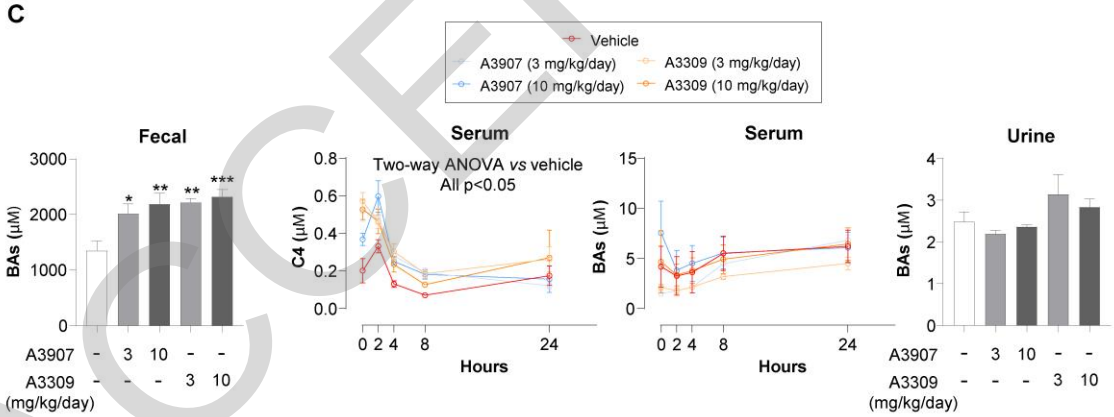

D

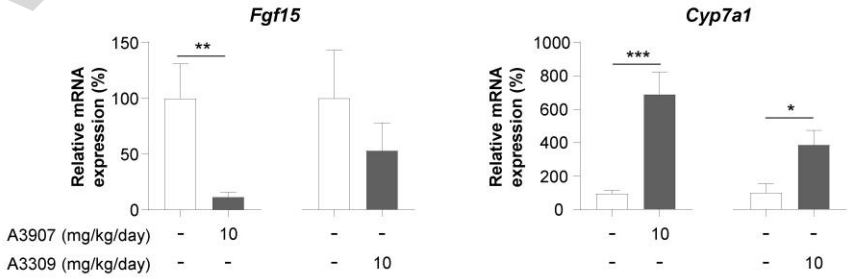

Figure 2. Therapeutic and pharmacodynamic effects of A3907 in *Mdr2*$^{-/-}$ mice. (**A**) Schematic representation of the experimental design (n=11 on each group). (**B**) Circulating levels of A3907 in plasma 2 h post-administration at the 4th week of treatment. (**C**) Comparison of the terminal body weight relative to treatment initiation and liver- and spleen-to-body weight ratios of the animals at sacrifice. (**D**) Plasma levels of circulating liver enzymes. (**E**) Representative hematoxylin-eosin (H&E) and immunohistochemistry (IHC) images of liver sections and comparison of the relative area of cytokeratin-7 (CK7), galectin-3, and α-smooth muscle actin (α-SMA); Scale bar: 100 µm. (**F**) Hepatic content of hydroxyproline and monocyte chemoattractant protein-1 (MCP-1), and quantification of total BA concentration in serum, and urine of the *Mdr2*$^{-/-}$ mice. All statistical data represents comparison *vs* vehicle group. Parametric one-way ANOVA with Dunnett's post hoc test or non-parametric Kruskal-Wallis test followed by Dunn's multiple comparison test were used to assess significance depending on the distribution of the data. *p<0.05; **p<0.01 and ***p<0.001.

Downloaded from http://journals.lww.com/hep by BhDMf5ePHKav1zEoum1tQfN4a+kJLhEZgbsIHo4XMi0hCywCX1AWnYQp/IlQrHD3i3D0OdRyi7TvSFl4Cf3VC4/OAVpDDa8K2+Ya6H515kE= on 04/04/2023

ACCEPTED

Downloaded from http://journals.lww.com/hep by BhDMf5ePHKav1zEoum1tQfN4a+kJLhEZgbsIHo4XMi0hCywCX1AWnYQp/IlQrHD3i3D0OdRyi7TvSFl4Cf3VC4/OAVpDDa8K2+Ya6H515kE= on 04/04/2023

ACCEPTED

Figure 2

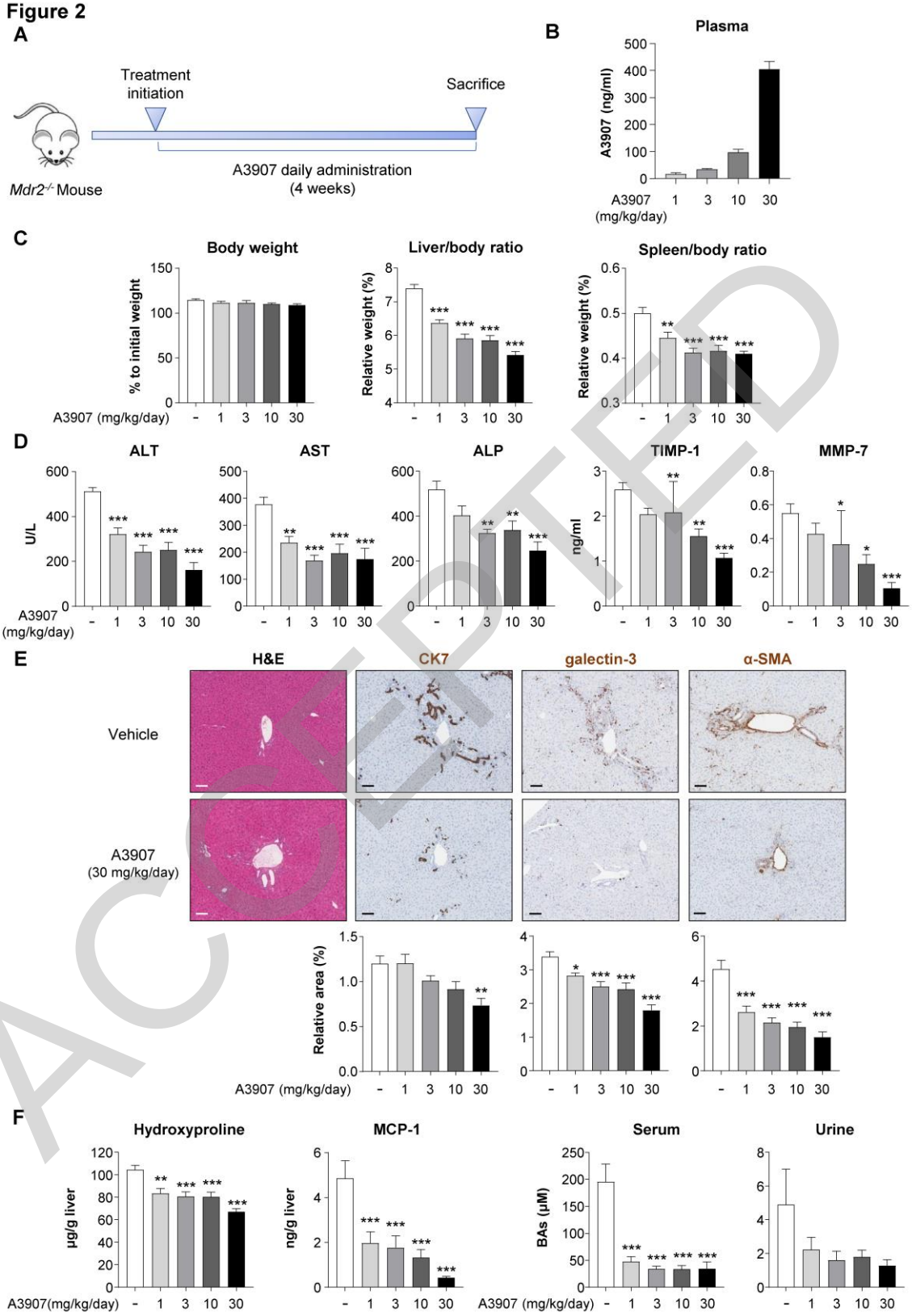

Figure 3. Hepatic transcriptome signatures in *Mdr2*$^{-/-}$ mice after A3907 treatment and cytoprotective effects of A3907 in cultured cholangiocytes.

(A) Quantification of the amount of apoptotic cell death analyzed by flow cytometry with Annexin V and To-PRO^{TM}-3 dual staining after incubating normal rat cholangiocytes (NRCs) with vehicle, glycochenodeoxycholic acid (GCDCA (1 mM)), Puromycin (4 □M), A3907 (1 □M), or combinations for 48 h. (**B**) Heatmap displaying the hepatic expression of genes significantly normalized (compared to WT mice) by A3907 (3 mg/kg/day) (108 upregulated and 335 downregulated by A3907 compared to vehicle) in *Mdr2*$^{-/-}$ mice by RNAseq analysis. (**C**) GO enrichment analysis of genes significantly modulated by A3907. (**D**) Heatmap representation of the differentially expressed genes annotated for each biological process. (**E**) Bar graph representation showing A3907-induced suppression of hepatic *S1pr2* overexpression in *Mdr2*$^{-/-}$ mice. For statistical analysis of flow cytometry data parametric one-way ANOVA with Dunnett's post hoc test was used to assess significance. **p*<0.05; ***p*<0.01 and ****p*<0.001. Gene set analysis was conducted with the R package PIANO version 1.18.1 using the Stouffer method, and p-values were corrected for multiple testing using the Benjamini-Hochberg method (False Discovery Rate, p<0.05).

Downloaded from http://journals.lww.com/hep by BhDMf5ePHKav1zEoum1tQfN4a+kJLhEZgbsIHo4XMi0hCywCX1AWnYQp/IlQrHD3i3D0OdRyi7TvSFl4Cf3VC4/OAVpDDa8K2+Ya6H515kE= on 04/04/2023

ACCEPTED

Downloaded from http://journals.lww.com/hep by BhDMf5ePHKav1zEoum1tQfN4a+kJLhEZgbsIHo4XMi0hCywCX1AWnYQp/IlQrHD3i3D0OdRyi7TvSFl4Cf3VC4/OAVpDDa8K2+Ya6H515kE= on 04/04/2023

ACCEPTED

Figure 3

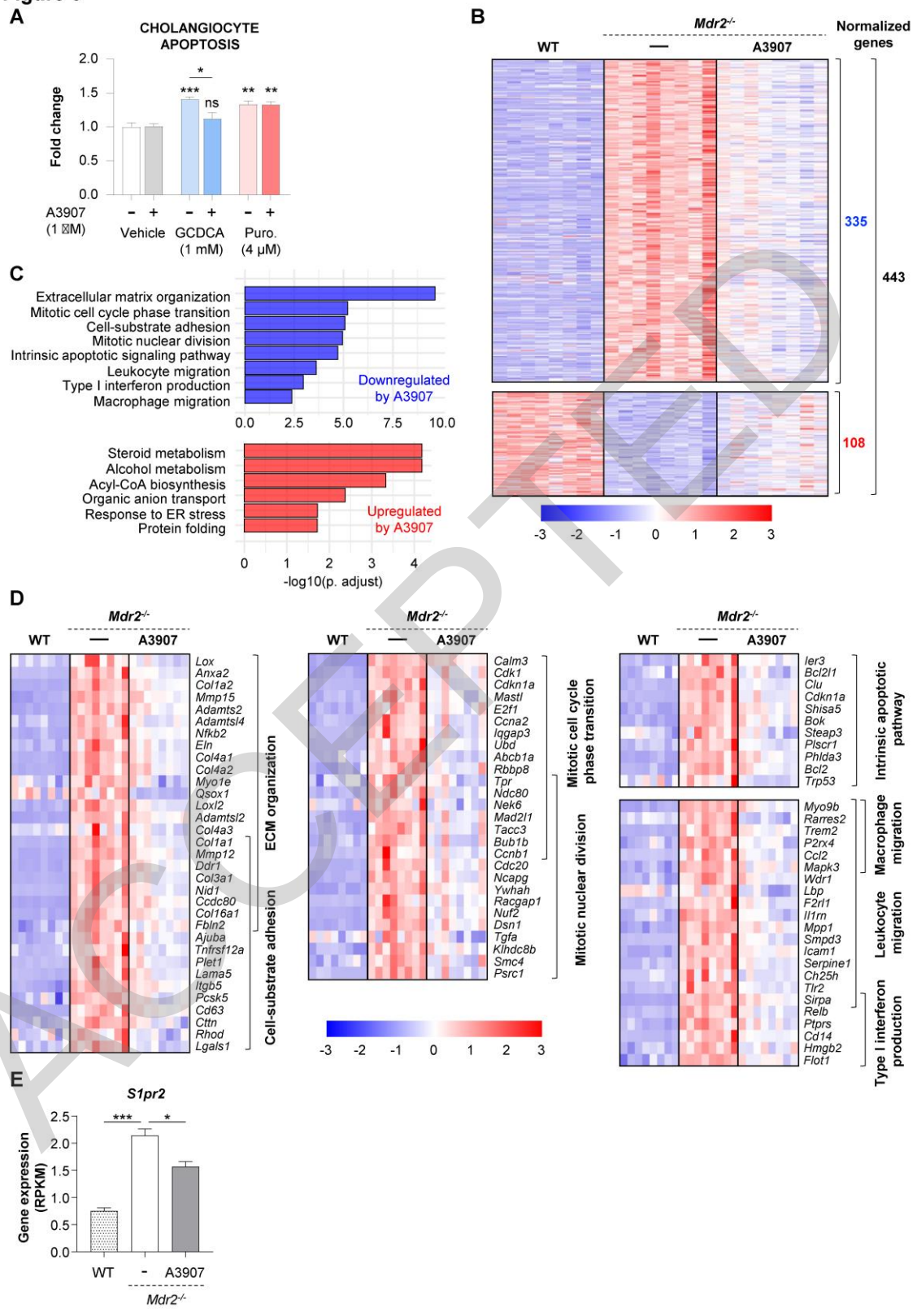

Downloaded from http://journals.lww.com/hep by BhDMf5ePHKav1zEoum1tQfN4a+kJLhEZgbsIHo4XMi0hCywCX1AWnYQp/IlQrHD3i3D0OdRyi7TvSFl4Cf3VC4/OAVpDDa8K2+Ya6H515kE= on 04/04/2023

Figure 4. Therapeutic and pharmacodynamic effects of A3907 in mice subjected to bile duct ligation (BDL). (**A**) Schematic representation of the experimental design (n=24 for vehicle and A3907 30 mg/kg groups, n=14 for A3907 3 mg/kg group, and n=12 for A3907 10 mg/kg group). (**B**) Terminal serum and bile concentrations of A3907 24 h post-administration of the last dose. (**C**) Representative whole-liver images and comparative body weight changes overtime, and terminal liver-to-body weight ratio. (**D**) Representative H&E images of liver sections and blinded scoring of inflammation and necrosis performed by an independent expert pathologist; Scale bar: 100 µm. (**E**) Total serum, bile and urine BA levels at sacrifice in mice subjected to BDL after daily treatment with A3907 for 11 days, and correlation analysis of serum *vs* urine BA levels in individual animals. Dashed lines represent comparison between A3907 grouped doses and vehicle-administered BDL mice. (**F**) Serum biochemical parameters at sacrifice. Values are represented as mean (SEM). ND, not detected. For statistical analysis of the histopathological scoring Mann-Whitney test was applied. Statistical analysis of body weight change overtime was performed by two-way ANOVA with Tukey's multiple comparisons post hoc test. For statistical analysis of individual doses *vs* vehicle, parametric one-way ANOVA with Dunnett's post hoc test or non-parametric Kruskal-Wallis test followed by Dunn's multiple comparison test were used depending on the normality of the data. For comparisons between A3907 group *vs* vehicle and sham *vs* vehicle, student´s t-test or Mann-Whitney test was applied depending on the distribution of the data. For correlation analysis Spearman test was applied. *p<0.05; **p<0.01 and ***p<0.001. *Abbreviations*: S, sham; -, vehicle.

ACCEPTED

Downloaded from http://journals.lww.com/hep by BhDMf5ePHKav1zEoum1tQfN4a+kJLhEZgbsIHo4XMi0hCywCX1AWnYQp/IlQrHD3i3D0OdRyi7TvSFl4Cf3VC4/OAVpDDa8K2+Ya6H515kE= on 04/04/2023

Figure 4

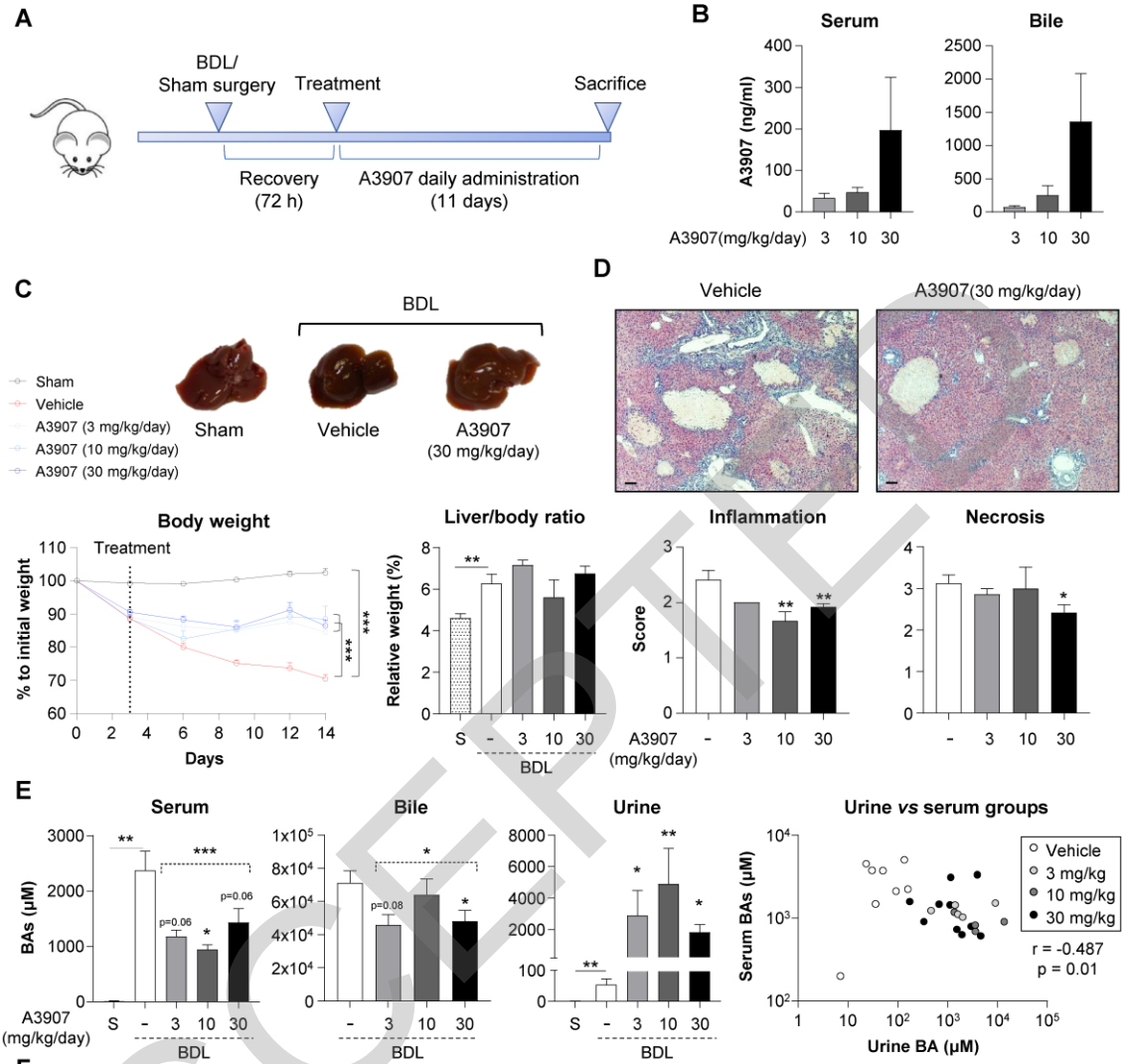

F

	(A)	(B)	A3907 (mg/kg/day) (C)			p value
	Sham	Vehicle	3	10	30	B *vs* C
ALT (U/L)	69.3 (21.7)***	472.3 (47.8)	234.7 (18.2)*	392.8 (69.5)	319.4 (46.1)*	**
AST (U/L)	267.4 (41.7)***	833.5 (87.5)	404 (39.2)**	631.2 (86.7)	525.7 (56.1)**	***
ALP (U/L)	132.6 (8.3)***	805.5 (93.0)	912.7 (102)	832.8 (162.5)	761.7 (72.1)	ns
Bilirubin (Total) (mg/dl)	ND	21.33 (2.79)	18.8 (1.33)	16.24 (2.62)	16.21 (1.325)	*
Bilirubin (Direct) (mg/dl)	ND	21.65 (2.44)	18.33 (1.34)	15.84 (2.62)	15.98 (1.3)	*
Bilirubin (Indirect) (mg/dl)	ND	1.4 (0.28)	0.47 (0.12)*	0.4*	0.4 (0.087)***	**
Albumin (g/dl)	3.7 (0.1)***	2.8 (0.2)	3.067 (0.1)	2.9 (0.2)	3.1 (0.1)	**
Urea (mg/dl)	45.1 (2.6)***	176 (24.6)	48.67 (5.9)***	85.6 (34.6)**	56.7 (7.2)***	***
Glucose (mg/dl)	284 (15.3)***	110.8 (11.9)	176 (11.6)**	165.6 (31)	156.4 (7.7)*	***
Triglycerides (mg/dl)	82.9 (15.0)	105.3 (10.9)	132.7 (13.7)	114.4 (21.6)	124 (9.5)	*
Cholesterol (mg/dl)	102.9 (11.4)***	557.5 (72.3)	278 (17.4)*	260 (54.5)*	306.7 (44.8)**	***
LDL (mg/dl)	ND	487.3 (73.2)	182 (18.4)*	180 (45.7)*	231.8 (43.0)**	***
HDL (mg/dl)	70.3 (8.8)*	47.8 (4.8)	70.67 (4)	57.6 (9.4)	62.1 (3.2)	**

ACCEPTED

Figure 5. Comparative analysis of the pharmacokinetics, pharmacodynamics and therapeutic effects of A3907 and A3309 in BDL mice. (**A**) Pharmacokinetic analysis of A3907 and A3309 in BDL mice administered with 3 and 10 mg/kg daily oral doses for 7 days. (**B**) Total BA levels at sacrifice in serum, bile and urine after daily treatment with either A3907 or A3309 (3 mg/kg/day) or vehicle for 11 days in mice subjected to BDL. (**C**) Body weight loss overtime in sham and BDL mice receiving A3907 or A3309 (3 mg/kg/day) or vehicle. (**D**) Levels of transaminases (ALT and AST) and urea in the different experimental groups at sacrifice. For statistical analysis student´s t-test or Mann-Whitney test was applied depending on the distribution of the data. Statistical analysis of body weight loss overtime was performed by two-way ANOVA with Tukey's multiple comparisons post hoc test. *p<0.05; **p<0.01 and ***p<0.001. *Abbreviations*: S, sham; -, vehicle.

Downloaded from http://journals.lww.com/hep by BhDMf5ePHKav1zEoum1tQfN4a+kJLhEZgbsIHo4XMi0hCywCX1AWnYQp/IlQrHD3i3D0OdRyi7TvSFl4Cf3VC4/OAVpDDa8K2+Ya6H515kE= on 04/04/2023

ACCEPTED

Figure 5

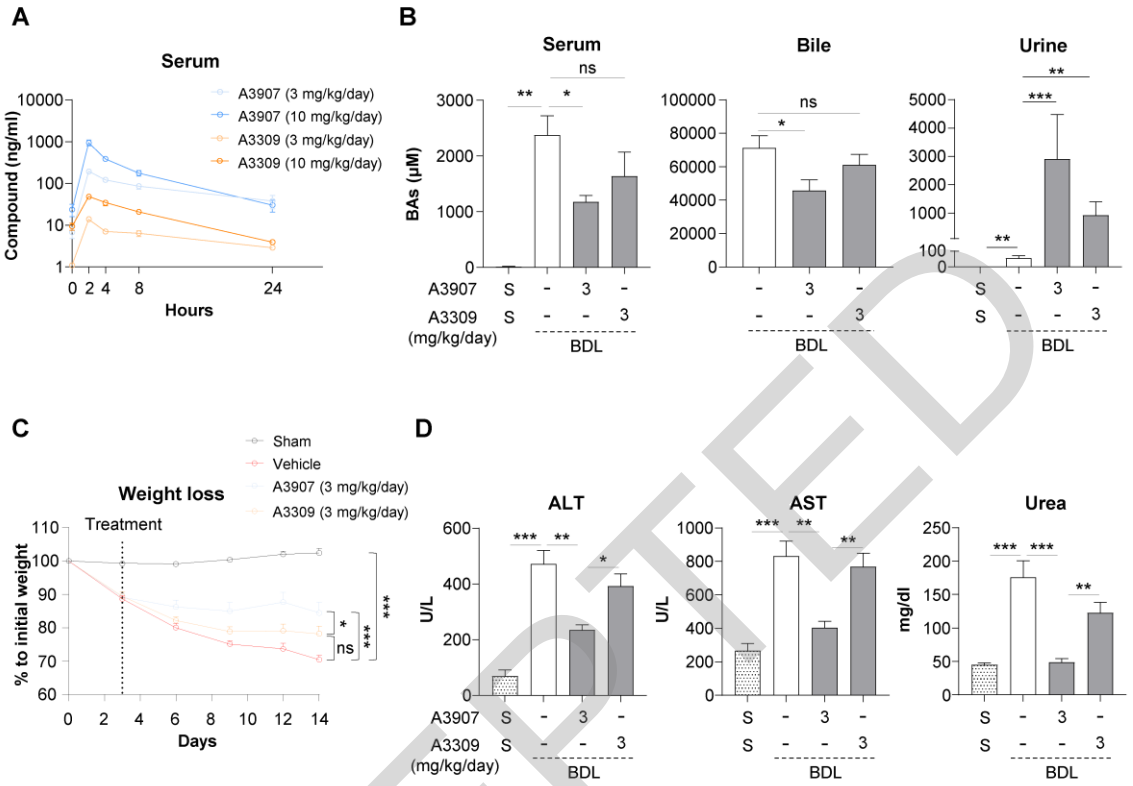

ACCEPTED

Downloaded from http://journals.lww.com/hep by BhDMf5ePHKav1zEoum1tQfN4a+kJLhEZgbsIHo4XMi0hCywCX1AWnYQp/IlQrHD3i3D0OdRyi7TvSFl4Cf3VC4/OAVpDDa8K2+Ya6H515kE= on 04/04/2023

Figure 6. Comparison of hepatic transcriptome signatures of A3907 and A3309 treatment in BDL mice. (**A**) Heatmap illustrating genes significantly normalized by A3907 (3 mg/kg/day) (126 upregulated and 177 downregulated by A3907). (**B**) GO enrichment analysis of genes significantly normalized by A3907. (**C**) Heatmaps representing the expression of individual genes annotated for each biological process. (**D**) Hepatic expression of *Nr1I2 and Slc51b* analyzed by RNAseq. Gene set analysis was conducted with the R package PIANO version 1.18.1 using the Stouffer method, and p-values were corrected for multiple testing using the Benjamini-Hochberg method (False Discovery Rate, $p<0.05$).

Downloaded from http://journals.lww.com/hep by BhDMf5ePHKav1zEoum1tQfN4a+kJLhEZgbsIHo4XMi0hCywCX1AWnYQp/IlQrHD3i3D0OdRyi7TvSFl4Cf3VC4/OAVpDDa8K2+Ya6H515kE= on 04/04/2023

ACCEPTED

Downloaded from http://journals.lww.com/hep by BhDMf5ePHKav1zEoum1tQfN4a+kJLhEZgbsIHo4XMi0hCywCX1AWnYQp/IlQrHD3i3D0OdRyi7TvSFl4Cf3VC4/OAVpDDa8K2+Ya6H515kE= on 04/04/2023

ACCEPTED

Figure 6

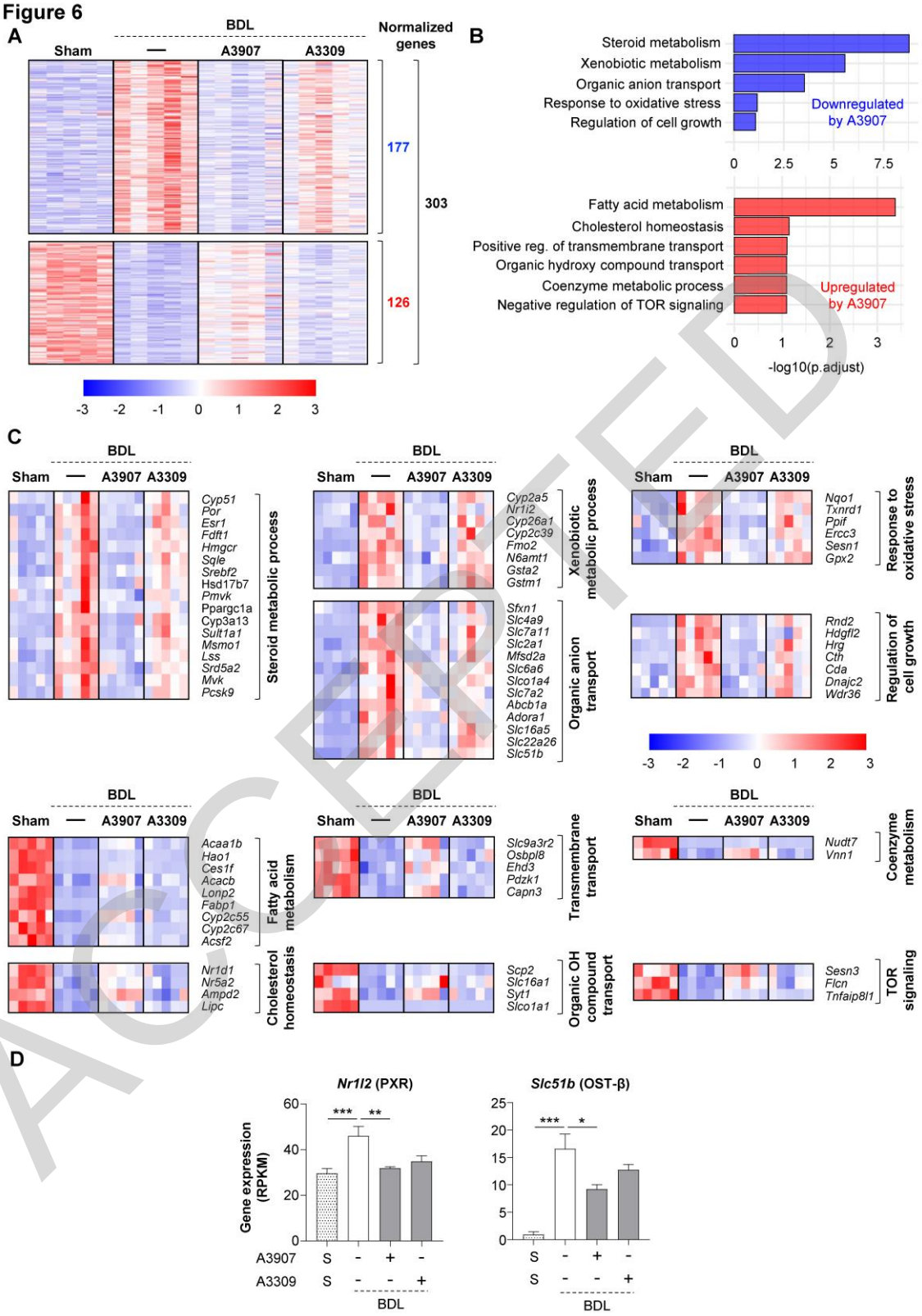

Downloaded from http://journals.lww.com/hep by BhDMf5ePHKav1zEoum1tQfN4a+kJLhEZgbsIHo4XMi0hCywCX1AWnYQp/IlQrHD3i3D0OdRyi7TvSFl4Cf3VC4/OAVpDDa8K2+Ya6H515kE= on 04/04/2023

Figure 7. Pharmacokinetic profile and pharmacological effects of A3907 in healthy subjects subjected to multiple ascending doses (MAD). (**A**) MAD study design. Healthy subjects were randomized into 3 different groups [group B1: 9 mg/day (A3907 n=6, placebo n=2); group B2: 27 mg/day (A3907 n=5, placebo n=1); group B3: 67.5 mg/day (A3907 n=6, placebo n=2)] and were administered one single oral dose of A3907 every 24 h for 7 days. Daily dose was administered after 10 h of fasting, and first meal was given 4.5 h after A3907 administration. (**B**) Plasma pharmacokinetic profile in healthy subjects at day 7. Values are expressed as Mean □ standard deviation (SD). *Abbreviations*: AUC_{inf}, AUC from the time of dosing to the last measurable concentration and extrapolated to infinity; C_{max}, maximum plasma concentrations; $t_{1/2}$, terminal half-life; T_{max}, time to reach the maximum concentrations. (**C**) Pharmacological effect of A3907. Time profile of plasma total BA and C4 concentrations over the last 24 h dosing interval. Post-prandial (6 h) plasma concentrations of total, unconjugated and conjugated BAs relative to baseline. (**D**) Comparison of circulating levels of A3907 in *Mdr2*$^{-/-}$ and BDL mice and human healthy subjects, as well as A3309 in BDL mice and human healthy subjects. AUC values in the *Mdr2*$^{-/-}$ mice are approximations calculated from pharmacokinetic data in C57BL/6J and CD-1 mice assuming comparable ADME profile. Statistical analysis of plasma BAs and C4 levels overtime was performed by two-way ANOVA with Tukey's multiple comparisons post hoc test. For statistical analysis of postprandial BA levels parametric one-way ANOVA with Dunnett's post hoc test was used. *p<0.05; **p<0.01 and ***p<0.001.

ACCEPTED

Downloaded from http://journals.lww.com/hep by BhDMf5ePHKav1zEoum1tQfN4a+kJLhEZgbsIHo4XMi0hCywCX1AWnYQp/IlQrHD3i3D0OdRyi7TvSFl4Cf3VC4/OAVpDDa8K2+Ya6H515kE= on 04/04/2023

Figure 7

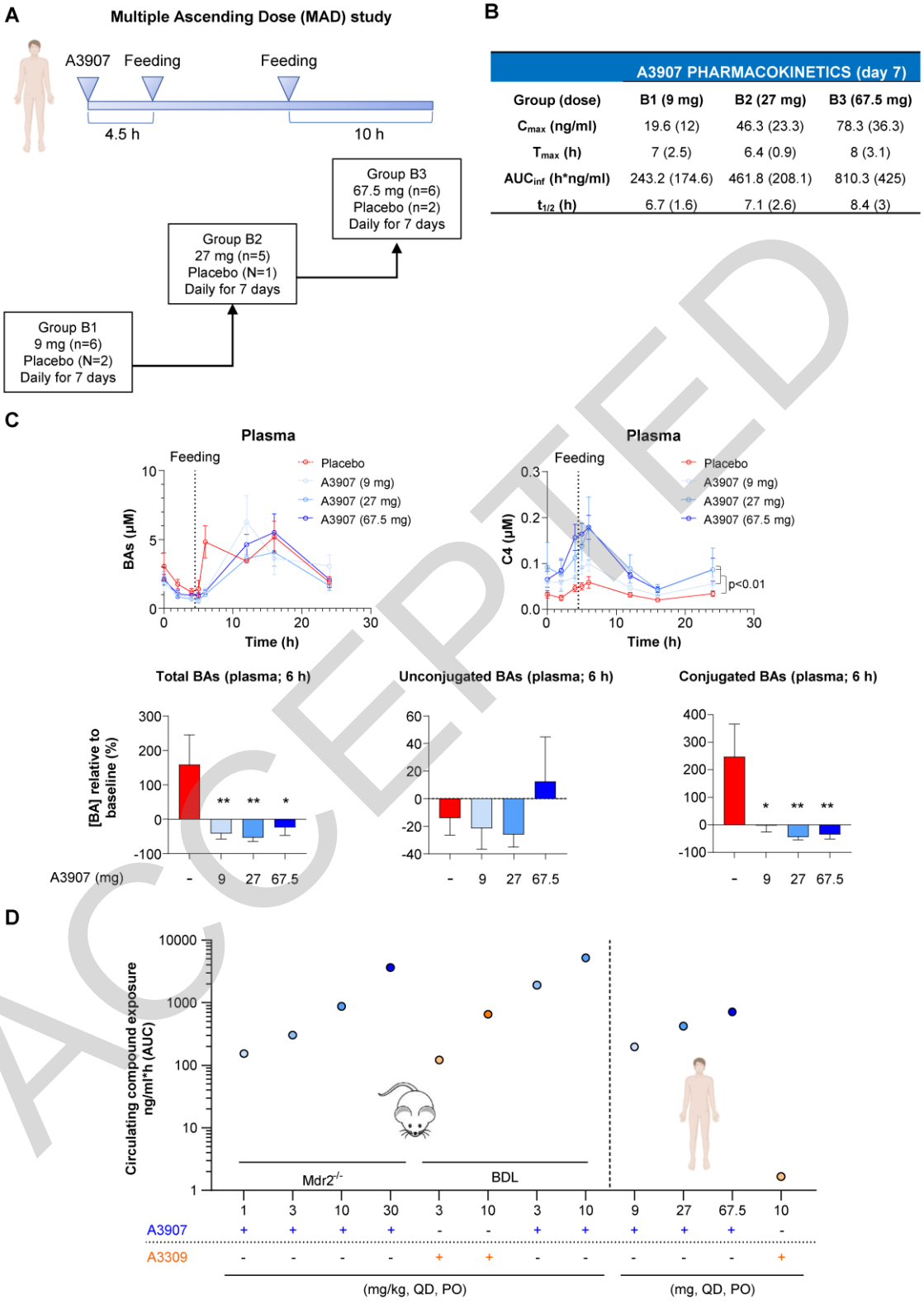

ACCEPTED